Tensor-multi-scalar theories: relativistic stars and 3+1 decomposition

Michael Horbatsch[1,2]**, Hector O. Silva**[2]**, Davide Gerosa**[3]**, Paolo Pani**[4,5]**, Emanuele Berti**[2,5]**, Leonardo Gualtieri**[4] **and Ulrich Sperhake**[2,3,6]

[1]School of Mathematical Sciences, University of Nottingham, Nottingham, NG7 2RD, UK
[2] Department of Physics and Astronomy, The University of Mississippi, University, MS 38677-1848, USA
[3] Department of Applied Mathematics and Theoretical Physics, Centre for Mathematical Sciences, University of Cambridge, Wilberforce Road, Cambridge CB3 0WA, UK
[4] Dipartimento di Fisica, "Sapienza" Università di Roma & Sezione INFN Roma 1, P.le A. Moro 2, 00185 Roma, Italy
[5] CENTRA, Departamento de Física, Instituto Superior Técnico, Universidade de Lisboa, Avenida Rovisco Pais 1, 1049 Lisboa, Portugal
[6] Theoretical Astrophysics 350-17, California Institute of Technology, Pasadena, CA 91125, USA

E-mail: `michael.horbatsch@nottingham.ac.uk`

Abstract. Gravitational theories with multiple scalar fields coupled to the metric and each other — a natural extension of the well studied single-scalar-tensor theories — are interesting phenomenological frameworks to describe deviations from general relativity in the strong-field regime. In these theories, the N-tuple of scalar fields takes values in a coordinate patch of an N-dimensional Riemannian target-space manifold whose properties are poorly constrained by weak-field observations. Here we introduce for simplicity a non-trivial model with two scalar fields and a maximally symmetric target-space manifold. Within this model we present a preliminary investigation of spontaneous scalarization for relativistic, perfect fluid stellar models in spherical symmetry. We find that the scalarization threshold is determined by the eigenvalues of a symmetric scalar-matter coupling matrix, and that the properties of strongly scalarized stellar configurations additionally depend on the target-space curvature radius. In preparation for numerical relativity simulations, we also write down the $3 + 1$ decomposition of the field equations for generic tensor-multi-scalar theories.

Contents

1. Introduction

Modifications of general relativity (GR) often lead to the introduction of additional degrees of freedom [1]. The simplest and best studied extension of GR is scalar-tensor (ST) theory, in which one or more scalar fields are included in the gravitational sector of the action through a non-minimal coupling between the Ricci scalar and a function of the scalar field(s). A further motivation to study ST theories is that they appear in different contexts in high-energy physics: they can be obtained as the low-energy limit of string theories [2], in Kaluza-Klein-like models [3] or in braneworld scenarios [4,5]. Moreover, ST theories play an important role in cosmology [6].

Almost 60 years ago, in an attempt to implement Mach's ideas in a relativistic theory of gravity, Jordan, Fierz, Brans and Dicke proposed a specific ST theory (commonly referred to as "Brans-Dicke theory") as a possible modification of GR [7–9]. Their theory is still viable, but it has since been constrained to be extremely close to GR by Solar System and binary pulsar observations [10]. Brans-Dicke theory was generalized by Bergmann and Wagoner, who considered the most general ST theory with a single scalar field and an action at most quadratic in derivatives of the fields [11,12]. In 1992 Damour and Esposito-Farèse introduced and investigated tensor-multi-scalar (TMS) theory, a generalization of the Bergmann-Wagoner theory to an arbitrary number of scalar fields [13]. Multiple scalar degrees of freedom are a generic prediction of string theories and theories involving extra dimensions (see e.g. [14–17]). In recent years, Bergmann-Wagoner theory has been extensively studied in the case of a single scalar field (see e.g. [18–21] and references therein). In comparison, very limited attention has been devoted to the phenomenological implications of TMS theory.

Even in the simplest case of a single scalar, ST theories give rise to interesting phenomenology. Although their action is linear in the curvature tensor, and scalar-matter couplings are highly constrained by observational bounds from the Solar System [22], ST theories can modify the strong-field regime of GR. Indeed, the equations of structure describing compact stars can admit non-perturbative solutions where the scalar fields can have large amplitudes [23]. This phenomenon, called *spontaneous scalarization*, can significantly affect the masses and radii of neutron stars. Spontaneous scalarization is strongly constrained by binary pulsar observations [24], but it could still leave a signature in the late inspiral of compact binaries through the so-called "dynamical scalarization" [25–27], which may be observable by advanced gravitational-wave detectors [28, 29].

In this article we study the phenomenology of TMS theories. The importance of our work for black hole physics is to a significant extent of indirect nature. Stellar collapse represents, of course, one of the most important channels for black hole formation, and ST theories of gravity are more likely to produce experimental signatures during black hole formation than in the dynamics of the remnant "quiescent" black hole spacetimes [30, 31]. The reason is that there are strong no-hair theorems∗ implying that stationary, vacuum black hole solutions in ST and TMS theories must be identical to GR (cf. [13,34–38] and Sotiriou's contribution to the present volume [39]). In addition, it has been shown that the dynamics of black-hole binaries in ST theory is undistinguishable from that in GR up to 2.5 post-Newtonian order [40,41] or – in the case of extreme mass-ratio – to all post-Newtonian orders [42]. This result does

---

∗ Hairy black hole solutions are possible in presence of a complex scalar field (i.e. two real scalar fields), as long as its phase is time-dependent [32]. No-hair theorems can also be evaded if the potential is non-convex; in this case the solutions are unstable, but their growth time can be extremely large [33].

not apply in the presence of non-trivial boundary conditions [43–45], but in this case violations of the no-hair theorem would most likely be unobservable. Nevertheless, black hole binaries have been studied in the framework of single-scalar theories using numerical relativity (cf. [44,45]), and the extension of such studies to TMS theories may still reveal surprising discoveries.

In order to pave the way for numerical investigations of black holes and neutron stars in TMS theories, in Section 4 we write down the TMS field equations in a 3+1 formalism that is suitable for numerical evolutions of compact binary systems.

A promising avenue to understand the experimental implications of TMS theories (following the reasoning of [23,46]) is to focus first on the coupling between the various scalars and matter. The scalar fields take values in a coordinate patch of a Riemannian *target-space* manifold. It is natural to ask whether this additional geometric structure can leave a detectable signature in compact stars and/or in the late inspiral of compact binaries, while still allowing for solutions compatible with binary pulsar observations.

This paper is a preliminary investigation in this direction. We will mainly focus on a simple non-trivial TMS model with two scalar fields and a vanishing potential. This model contains the main novel features that distinguish TMS theories from single-scalar theories, i.e. the presence of a target-space manifold with non-trivial Riemannian structure and non-vanishing curvature, and the presence of a continuous symmetry that is spontaneously broken by scalarized solutions. A more systematic study of scalarization in this prototype TMS theory will be the topic of a future publication, and it should give us useful insight into strong-field effects that characterize more general TMS theories.

The plan of the paper is as follows. In Section 2 we introduce the action and the field equations of TMS theory. We then specialize the field equations to the case of two scalar fields with vanishing potential and a maximally symmetric target-space manifold. In Section 3 we derive the equations for slowly rotating relativistic stars, and we perform numerical integrations of these equations in the non-rotating case. In Section 4 we derive the $3 + 1$ decomposition of the TMS field equations, which can be used to perform fully non-linear numerical evolutions. In Section 5 we draw some conclusions and point out possible directions for future work. The Appendices contain some technical material on the structure of target spaces in our model (Appendix A), experimental constraints (Appendix B) and perturbative arguments to predict the spontaneous scalarization threshold in models with two scalar fields (Appendix C).

2. Tensor-multi-scalar theories: action, field equations, scalar-matter couplings, and symmetries

2.1. Units, notation and conventions

Throughout the paper we use units with $c = 1$. The gravitational constant measured in a Cavendish experiment is denoted by G, while the "bare" gravitational constant appearing in the action is denoted by $G_\star$: the relation between the two constants is written down explicitly in Eq. (B.1). Indices on space-time tensors are denoted by Greek letters and take values $0, \ldots, 3$, and space-time coordinates are denoted by x^μ. The Lorentzian space-time metric is taken to have signature $(-, +, +, +)$, and its components are denoted by $g_{\mu\nu}(x)$. The conventions for the Riemann curvature tensor and its contractions, as well as the notation for symmetrization and anti-symmetrization of tensors, are those of Misner, Thorne, and Wheeler [47].

The N-tuple of scalar fields $\varphi^A(x) = (\varphi^1(x), \ldots, \varphi^N(x))$ takes values in a coordinate patch of an N-dimensional Riemannian target-space manifold. Indices on target-space tensors are denoted by early capital Roman letters A, B, C, $\ldots$, and take integer values $1, \ldots, N$. Components of the Riemannian target-space metric are denoted by $\gamma_{AB}(\varphi)$, and the associated Christoffel symbols are denoted by $\gamma^C{}_{AB}(\varphi)$. The target-space Riemann curvature tensor is denoted by $\mathcal{R}^A{}_{BCD}(\varphi)$, with obvious notation for derived quantities such as the Ricci tensor and the Ricci scalar. If the target space has a Hermitian structure∗, then indices on complexified tensors are denoted by lower-case Roman letters, and take values $1, 2, \ldots, N/2$. Holomorphic coordinates are denoted by $(\varphi^a, \bar{\varphi}^a)$, and the components of the Hermitian metric in these coordinates are denoted by $\gamma_{\bar{a}b}(\varphi, \bar{\varphi})$. For reference, in Table 1 we provide an overview of the meaning of the various symbols and conventions used in this paper.

2.2. Action and field equations for N real scalars

We consider a gravitational theory with metric tensor $g_{\mu\nu}$, and scalar fields $\varphi^1, \ldots, \varphi^N$ which take values in a coordinate patch of an N-dimensional target-space manifold. We assume that all non-gravitational fields, denoted collectively by Ψ, couple only to the Jordan-frame metric $\tilde{g}_{\mu\nu} = A^2(\varphi)g_{\mu\nu}$, so that the matter action has the functional form $S_{\mathrm{m}}[\Psi; \tilde{g}_{\mu\nu}]$. This assumption guarantees that the Weak Equivalence Principle (WEP), which has been experimentally verified with great accuracy [10], will hold. The quantity $A(\varphi)$ is a conformal factor relating the metrics $\tilde{g}_{\mu\nu}$ and $g_{\mu\nu}$.

The most general action which is invariant under space-time and target-space diffeomorphisms (up to boundary terms and field redefinitions), and has at most two space-time derivatives, can be written in the form [13]

$$S = \frac{1}{4\pi G_\star} \int d^4x \sqrt{-g} \left[\frac{R}{4} - \frac{1}{2}g^{\mu\nu}\gamma_{AB}(\varphi)\partial_\mu\varphi^A\,\partial_\nu\varphi^B - V(\varphi) \right] + S_{\mathrm{m}}[A^2(\varphi)g_{\mu\nu}; \Psi],$$

(2.1)

where $G_\star$ is a bare gravitational constant, and g and R are the determinant and Ricci scalar of $g_{\mu\nu}$, respectively. The positive-definiteness of the target-space Riemannian metric $\gamma_{AB}(\varphi)$ guarantees the absence of negative-energy excitations. The scalars φ^A are dimensionless and the potential $V(\varphi)$ has length dimensions minus two. The conformal factor $A(\varphi)$ is dimensionless. In the case of a single scalar ($N = 1$), the target-space metric $\gamma_{AB}(\varphi)$ reduces to a scalar function $\gamma(\varphi)$, and the choice $\gamma(\varphi) = 1$ can be made without loss of generality.

The field equations of the theory, obtained by varying the action (2.1) with respect to $g^{\mu\nu}$ and φ, take the form

$$R_{\mu\nu} = 2\gamma_{AB}(\varphi)\nabla_\mu\varphi^A\nabla_\nu\varphi^B + 2V(\varphi)g_{\mu\nu} + 8\pi G_\star\left(T_{\mu\nu} - \frac{1}{2}Tg_{\mu\nu}\right),$$

(2.2)

$$\Box\varphi^A = -\gamma^A{}_{BC}(\varphi)g^{\mu\nu}\nabla_\mu\varphi^B\nabla_\nu\varphi^C + \gamma^{AB}(\varphi)\frac{\partial V(\varphi)}{\partial\varphi^B} - 4\pi G_\star\gamma^{AB}(\varphi)\frac{\partial\log A(\varphi)}{\partial\varphi^B}T.$$

(2.3)

Here ∇_μ is the covariant derivative associated with $g_{\mu\nu}$, and $\Box \equiv \nabla^\mu\nabla_\mu$ is the corresponding d'Alembertian operator. The Ricci tensor built out of the metric $g_{\mu\nu}$

∗ For an introduction to Hermitian structures and complex differential geometry, see e.g. [48].

G	Gravitational constant from a Cavendish experiment
$G_\star$	Bare gravitational constants appearing in the action
μ, ν, ρ	Spacetime indices
x^μ	Spacetime coordinates
$g_{\mu\nu}$	Spacetime metric in the Einstein frame
∇_μ	Covariant derivative associated with $g_{\mu\nu}$
$R^\mu{}_{\nu\rho\sigma}$	Spacetime Riemann tensor
A, B, C	Scalar-field indices in real notation
N	Number of scalar fields
φ^A	Gravitational scalar fields in real notation
γ_{AB}	Target-space metric in real notation
γ^A_{BC}	Christoffel symbols on the target space in real notation
$\mathcal{R}^A{}_{BCD}$	Target-space Riemann tensor
Ψ	Non-gravitational fields
$\tilde{g}_{\mu\nu}$	Spacetime metric in the Jordan frame
$A(\varphi)$	Einstein-Jordan frame conformal factor
$V(\varphi)$	Scalar-field potential
a, b, c	Scalar-field indices in complex notation
$\varphi^a, \bar{\varphi}^a$	Gravitational scalar fields in complex notation
$\gamma_{\bar{a}b}$	Target-space metric in complex notation
$\gamma^a_{\bar{b}c},\ \gamma^a_{bc}$	Christoffel symbols on the target space in complex notation
$\mathfrak{r}$	Target-space curvature radius ($N = 2$)
$\kappa(\varphi, \bar{\varphi})$	Scalar-matter coupling function ($N = 2$), see Eq. (2.19)
$\alpha^*, \bar{\alpha}^*$	Linear-term coefficients in the expansion of $\log A(\psi, \bar{\psi})$
$\beta_0, \beta_1^*, \bar{\beta}_1^*$	Quadratic-term coefficients in the expansion of $\log A(\psi, \bar{\psi})$
θ	Generic rotation angle in the target-space complex plane
α, β_1	Redefinition of α^*, β_1^*, after rotation
$\psi, \bar{\psi}$	Redefinition of the fields $\varphi, \bar{\varphi}$ after rotation
Z	$\mathrm{Re}[\psi]$
W	$\mathrm{Im}[\psi]$
t, r, θ, ϕ	Spacetime coordinates for stellar models
$\nu(r)$	Lapse function
$m(r) = r\mu(r)$	Mass function
$\omega(r)$	Fluid differential angular velocity
Ω	Angular velocity of the star
ρ	Fluid mass-energy density
P	Fluid pressure
n_B	Baryon density
$u^\mu, \tilde{u}^\mu$	Fluid 4-velocity in the Einstein/Jordan frame
Subscript "0"	Previous quantities evaluated at the star's center, $r = 0$
$R, \tilde{R}$	Stellar radius in the Einstein/Jordan frame
ψ_∞	Asymptotic value of the scalar field
M	Gravitational mass of the star
Q	Scalar charge of the star
M_B	Baryonic mass of the star
K, n_0, m_b, γ	Equation of state parameters, see Eq. (3.17)

Table 1. Variables and conventions used in this paper. Quantities above the horizontal line define the theory; quantities below the horizontal line refer to stellar models.

is denoted as $R_{\mu\nu}$. The energy-momentum tensor $T_{\mu\nu}$ of the non-gravitational fields is defined by

$$T_{\mu\nu} \equiv -\frac{2}{\sqrt{-g}}\frac{\delta S_{\mathrm{m}}[A^2(\varphi)g_{\rho\sigma};\Psi]}{\delta g^{\mu\nu}}\,, \tag{2.4}$$

and its trace is given by $T \equiv g^{\mu\nu}T_{\mu\nu}$.

The energy conservation equation reads

$$\nabla^\mu\left[T_{\mu\nu} + T^{(\varphi)}_{\mu\nu}\right] = 0\,, \tag{2.5}$$

or, more explicitly,

$$\nabla^\mu T_{\mu\nu} = \frac{\partial \log A(\varphi)}{\partial \varphi^A}\,T\,\nabla_\nu\varphi^A\,. \tag{2.6}$$

Here

$$
\begin{aligned}
T^{(\varphi)}_{\mu\nu} &\equiv -\frac{2}{\sqrt{-g}}\frac{\delta S_\varphi[g_{\rho\sigma};\varphi]}{\delta g^{\mu\nu}} \\
&= \frac{1}{4\pi G_\star}\left[\gamma_{AB}(\varphi)\left(\nabla_\mu\varphi^A\nabla_\nu\varphi^B - \frac{1}{2}g_{\mu\nu}g^{\rho\sigma}\nabla_\rho\varphi^A\nabla_\sigma\varphi^B\right) - V(\varphi)g_{\mu\nu}\right]
\end{aligned} \tag{2.7}
$$

is an effective energy-momentum tensor for the scalar fields, where S_φ denotes the scalar kinetic and potential contributions to the action (2.1). One may build an energy-momentum tensor which is conserved with respect to the Levi-Civita connection of the Jordan-frame metric, and whose components are directly related to physically observable quantities as

$$\tilde{T}_{\mu\nu} \equiv -\frac{2}{\sqrt{-\tilde{g}}}\frac{\delta S_m[\tilde{g}_{\rho\sigma};\Psi]}{\delta \tilde{g}^{\mu\nu}} = A^{-2}(\varphi)T_{\mu\nu}\,. \tag{2.8}$$

2.3. Complexification

If the target space has a Hermitian structure, then it is useful to write the action in terms of holomorphic coordinates and complexified tensors:

$$
\begin{aligned}
S = \frac{1}{4\pi G_\star}\int d^4x\sqrt{-g}&\left[\frac{R}{4} - g^{\mu\nu}\gamma_{\bar{a}b}(\varphi,\bar{\varphi})\nabla_\mu\bar{\varphi}^a\,\nabla_\nu\varphi^b - V(\varphi,\bar{\varphi})\right] \\
&+ S_{\mathrm{m}}[A^2(\varphi,\bar{\varphi})g_{\mu\nu};\Psi]\,.
\end{aligned} \tag{2.9}
$$

The complexified field equations are:

$$R_{\mu\nu} = 4\gamma_{\bar{a}b}(\varphi,\bar{\varphi})\nabla_{(\mu}\bar{\varphi}^a\nabla_{\nu)}\varphi^b + 2V(\varphi,\bar{\varphi})g_{\mu\nu} + 8\pi G_\star\left(T_{\mu\nu} - \frac{1}{2}Tg_{\mu\nu}\right)\,, \tag{2.10}$$

$$
\begin{aligned}
\Box\varphi^a =\ &-\gamma^a{}_{bc}(\varphi,\bar{\varphi})g^{\mu\nu}\nabla_\mu\varphi^b\nabla_\nu\varphi^c - 2\gamma^a{}_{\bar{b}c}(\varphi,\bar{\varphi})g^{\mu\nu}\nabla_\mu\bar{\varphi}^b\nabla_\nu\varphi^c \\
&+ \gamma^{a\bar{b}}(\varphi,\bar{\varphi})\frac{\partial V(\varphi,\bar{\varphi})}{\partial\bar{\varphi}^b} - 4\pi G_\star\gamma^{a\bar{b}}(\varphi,\bar{\varphi})\frac{\partial\log A(\varphi,\bar{\varphi})}{\partial\bar{\varphi}^b}T\,.
\end{aligned} \tag{2.11}
$$

Note that for Kähler manifolds (and in particular one-complex-dimensional manifolds)

$$\gamma^a{}_{\bar{b}c}(\varphi,\bar{\varphi}) = 0\,, \qquad \gamma^a{}_{bc}(\varphi,\bar{\varphi}) = \gamma^{a\bar{d}}(\varphi,\bar{\varphi})\frac{\partial\gamma_{c\bar{d}}(\varphi,\bar{\varphi})}{\partial\varphi^b}\,, \tag{2.12}$$

so in this particular case the scalar field equations would simplify considerably.

2.4. A two-real-scalar model with maximally symmetric target space

The simplest extension of a ST theory with a single real scalar field is the case of two real scalar fields. We will mostly focus on this model to illustrate the basic features of the new phenomenology arising in TMS theories relative to the case of a single real scalar. If the target space is assumed to be maximally symmetric, then there are three possibilities for its geometry: flat, spherical, or hyperbolic. In the flat case, the target space may be trivially identified with the complex plane $\mathbb{C}$. In the spherical case, the target space may be conformally mapped to the one-point-compactification $\hat{\mathbb{C}}$ of the complex plane $\mathbb{C}$ by means of stereographic projection. In the case of a hyperboloid of two sheets, the target space may be conformally mapped to $\hat{\mathbb{C}} \backslash S^1$, also by means of stereographic projection (we shall neglect the case of a hyperboloid of one sheet); see Appendix A for details. Using the complex formulation discussed in Section 2.3, we work with a single complex scalar rather than two real scalars, for which the action (2.9) reduces to

$$S = \frac{1}{4\pi G_\star} \int d^4x \sqrt{-g} \left[\frac{R}{4} - g^{\mu\nu} \gamma(\varphi, \bar{\varphi}) \nabla_\mu \bar{\varphi} \nabla_\nu \varphi - V(\varphi, \bar{\varphi}) \right] + S_{\mathrm{m}}[A^2(\varphi, \bar{\varphi})g_{\mu\nu}; \Psi],$$

(2.13)

and the field equations are

$$R_{\mu\nu} = 4\gamma(\varphi, \bar{\varphi}) \nabla_{(\mu} \bar{\varphi} \nabla_{\nu)} \varphi + 2V(\varphi, \bar{\varphi})g_{\mu\nu} + 8\pi G_\star \left(T_{\mu\nu} - \frac{1}{2}Tg_{\mu\nu} \right),$$

(2.14)

$$\Box\varphi = -\frac{\partial \log \gamma(\varphi, \bar{\varphi})}{\partial \varphi} g^{\mu\nu} \nabla_\mu \varphi \nabla_\nu \varphi + \gamma^{-1}(\varphi, \bar{\varphi}) \frac{\partial V(\varphi, \bar{\varphi})}{\partial \bar{\varphi}}$$
$$- 4\pi G_\star \gamma^{-1}(\varphi, \bar{\varphi}) \frac{\partial \log A(\varphi, \bar{\varphi})}{\partial \bar{\varphi}} T.$$

(2.15)

Hereafter we assume that the potential vanishes, i.e. $V(\varphi, \bar{\varphi}) = 0$, and that the target space is maximally symmetric. Therefore, upon stereographic projection and field redefinition (see Appendix A), the target-space metric can be written as

$$\gamma(\varphi, \bar{\varphi}) = \frac{1}{2} \left(1 + \frac{\bar{\varphi}\varphi}{4\mathbf{r}^2} \right)^{-2},$$

(2.16)

where $\mathbf{r}$ is the radius of curvature of the target-space geometry: for a spherical geometry we have $\mathbf{r}^2 > 0$, for a hyperbolic geometry $\mathbf{r}^2 < 0$, and in the limit $\mathbf{r} \to \infty$ the geometry is flat.

With the above choices, the field equations become

$$R_{\mu\nu} = 2 \left(1 + \frac{\bar{\varphi}\varphi}{4\mathbf{r}^2} \right)^{-2} \partial_{(\mu} \bar{\varphi} \partial_{\nu)} \varphi + 8\pi G_\star \left(T_{\mu\nu} - \frac{1}{2}Tg_{\mu\nu} \right),$$

(2.17)

$$\Box\varphi = \left(\frac{2\bar{\varphi}}{\bar{\varphi}\varphi + 4\mathbf{r}^2} \right) g^{\mu\nu} \partial_\mu \varphi \partial_\nu \varphi - 4\pi G_\star \left(1 + \frac{\bar{\varphi}\varphi}{4\mathbf{r}^2} \right) \bar{\kappa}(\varphi, \bar{\varphi}) T,$$

(2.18)

where we introduced

$$\kappa(\varphi, \bar{\varphi}) \equiv 2 \left(1 + \frac{\bar{\varphi}\varphi}{4\mathbf{r}^2} \right) \frac{\partial \log A(\varphi, \bar{\varphi})}{\partial \varphi},$$

(2.19)

the so-called scalar-matter coupling function.

The function $A(\varphi, \bar{\varphi})$, whose derivative enters into the field equations, determines the scalar-matter coupling through Eq. (2.19). Without loss of generality we assume that far away from the source the field vanishes, i.e. that the asymptotic value of the scalar field is $\varphi_\infty = 0$. We then expand the function $\log A$ in a series about $\varphi = 0$:

$$\log A(\varphi, \bar{\varphi}) = \alpha^* \varphi + \bar{\alpha}^* \bar{\varphi} + \frac{1}{2} \beta_0 \varphi \bar{\varphi} + \frac{1}{4} \beta_1^* \varphi^2 + \frac{1}{4} \bar{\beta}_1^* \bar{\varphi}^2 + \dots , \qquad (2.20)$$

where β_0 is real, while α^* and β_1^* are in general complex numbers∗. Although the five real parameters $\mathrm{Re}[\alpha^*], \mathrm{Im}[\alpha^*], \beta_0, \mathrm{Re}[\beta_1^*], \mathrm{Im}[\beta_1^*]$ are defined in terms of a specific target-space coordinate system, the four real quantities $(|\alpha^*|, \beta_0, |\beta_1^*|, \arg \alpha^* - \frac{1}{2} \arg \beta_1^*)$ may be expressed solely in terms of target-space scalar quantities, and thus have an invariant geometric meaning†. The remaining real parameter is an unmeasurable overall complex phase.

To make this explicit, redefine $\beta_1^* \equiv \beta_1 e^{i\theta}$, where θ is chosen such that β_1 is real. Then, after defining $\alpha^* \equiv \alpha e^{i\theta/2}$ and a new field $\psi \equiv \varphi e^{i\theta/2}$, the field equations become

$$R_{\mu\nu} = 2 \left(1 + \frac{\bar{\psi}\psi}{4\mathbf{r}^2}\right)^{-2} \partial_{(\mu}\bar{\psi}\partial_{\nu)}\psi + 8\pi G_\star \left(T_{\mu\nu} - \frac{1}{2} T g_{\mu\nu}\right) , \qquad (2.21)$$

$$\Box\psi = \left(\frac{2\bar{\psi}}{\bar{\psi}\psi + 4\mathbf{r}^2}\right) g^{\mu\nu} \partial_\mu \psi \partial_\nu \psi - 4\pi G_\star \left(1 + \frac{\bar{\psi}\psi}{4\mathbf{r}^2}\right) \bar{\kappa}(\psi, \bar{\psi}) T , \qquad (2.22)$$

where the function κ is defined in Eq. (2.19) and

$$\log A(\psi, \bar{\psi}) = \alpha\psi + \bar{\alpha}\bar{\psi} + \frac{1}{2}\beta_0 \psi\bar{\psi} + \frac{1}{4}\beta_1 \psi^2 + \frac{1}{4}\beta_1 \bar{\psi}^2 + \dots . \qquad (2.23)$$

Therefore, any solution of the original theory (formulated with respect to φ and complex coupling coefficients α^* and β_1^*) can be obtained from a theory where we consider the field ψ, a real-valued β_1 and a generically complex α. The solution for the theory corresponding to the conformal factor (2.20) is then given by a simple rotation, $\varphi = \psi \exp(-i\theta/2)$.

The model just described represents the simplest, yet quite comprehensive, generalization of the model of single ST theory investigated originally in Ref. [23].

Note that the quantity $|\alpha|^2 \equiv \alpha\bar{\alpha} \equiv \mathrm{Re}[\alpha]^2 + \mathrm{Im}[\alpha]^2$ is strongly constrained by observations (cf. Appendix B), similarly to the single-scalar case. When $\alpha = 0$, the conformal coupling reduces to

$$\log A(\psi, \bar{\psi}) = \frac{1}{2}\beta_0 \psi\bar{\psi} + \frac{1}{4}\beta_1 \psi^2 + \frac{1}{4}\beta_1 \bar{\psi}^2 , \qquad (2.24)$$

where we neglected higher-order terms in the scalar field. However, in TMS theories α is a complex quantity and its argument, $\arg \alpha$, is completely unconstrained in the weak-field regime. In Section 3.2.2 we will show that compact stars in theories with $\alpha = 0$ and $\alpha \neq 0$ are rather different.

∗ At the onset of spontaneous scalarization $|\varphi| \ll 1$, and we can always expand the conformal factor as in Eq. (2.20). For scalarized solutions the field amplitude may be large, the higher-order terms in the expansion may not be negligible, and the expansion (2.20) should be considered as an ansatz for the conformal factor. For a general functional form of the conformal factor, the series expansion used here (and in Ref. [23]) can only provide a qualitative description of the scalarized solution.

† The eigenvalues of the quadratic form in (2.20), given by $\beta_0 \pm |\beta_1^*|$, are target-space scalars. The phase difference $\arg \alpha^* - \frac{1}{2} \arg \beta_1^*$ arises when this quadratic form is contracted with α^*, see Eq. (B.6).

The field equations can be also written in terms of two real scalars. For this purpose, let us split the field ψ into real and imaginary parts: $\psi \equiv \mathrm{Re}[\psi] + \mathrm{i}\,\mathrm{Im}[\psi]$. Then the conformal factor (2.24), again in the $\alpha = \bar{\alpha} = 0$ case, reads:

$$\log A(\psi, \bar{\psi}) = \frac{1}{2} \left[(\beta_0 + \beta_1)\mathrm{Re}[\psi]^2 + (\beta_0 - \beta_1)\mathrm{Im}[\psi]^2 \right] . \tag{2.25}$$

The structure of this TMS theory is ultimately determined by three real parameters: $\beta_0 + \beta_1$, $\beta_0 - \beta_1$ and the target-space curvature defined by $\mathbf{r}^2$. When $\alpha \neq 0$, two further parameters ($|\alpha|$ and $\arg \alpha$) are necessary to define the theory.

3. Stellar structure in tensor-multi-scalar theories

In this section we consider the structure of relativistic stars in the context of the TMS theory introduced in Section 2.4. We first derive the equations of structure for a slowly rotating star in the Hartle-Thorne formalism [49, 50] (Section 3.1), then we integrate these equations and discuss some properties of scalarized solutions in increasingly complex scenarios (Section 3.2).

3.1. Equations of hydrostatic equilibrium

We describe a stationary, axisymmetric star, composed by a perfect fluid, slowly rotating with angular velocity Ω, using coordinates $x^\mu = (t, r, \theta, \phi)$ and the line element

$$\begin{aligned} g_{\mu\nu}dx^\mu dx^\nu &= -e^{\nu(r)}dt^2 + \frac{dr^2}{1 - 2\mu(r)} + r^2(d\theta^2 + \sin^2\theta d\phi^2) \\ &\quad + 2\left[\omega(r) - \Omega\right]r^2 \sin^2\theta dt d\phi. \end{aligned} \tag{3.1}$$

where we neglect terms of order $\sim \Omega^2$ and higher in the metric and in the hydrodynamical quantities. The variable $\mu(r)$ is related to the more familiar mass function $m(r)$ by $\mu = m/r$. The energy-momentum tensor of the perfect fluid takes the usual form

$$T^{\mu\nu} = A^4(\psi, \bar{\psi})\left[(\rho + P)u^\mu u^\nu + Pg^{\mu\nu}\right] , \tag{3.2}$$

where ρ, P, and $\tilde{u}^\mu = A^{-1}(\psi, \bar{\psi})u^\mu$ are the mass-energy density, pressure, and four-velocity of the fluid, respectively, and

$$u^\mu = e^{-\nu/2}(1, 0, 0, \Omega) . \tag{3.3}$$

With these choices, the field equations (2.2)–(2.3) reduce to a system of coupled ordinary differential equations, namely

$$(r\mu)' = \frac{1}{2}(1 - 2\mu)r^2 \left(1 + \frac{\bar{\psi}\psi}{4\mathfrak{r}^2}\right)^{-2} \bar{\psi}'\psi' + 4\pi G_\star A^4(\psi, \bar{\psi})r^2\rho \,, \tag{3.4}$$

$$P' = -(\rho c^2 + P)\left\{\frac{\nu'}{2} + \frac{1}{2}\left(1 + \frac{\bar{\psi}\psi}{4\mathfrak{r}^2}\right)^{-1} \left[\kappa(\psi, \bar{\psi})\psi' + \bar{\kappa}(\psi, \bar{\psi})\bar{\psi}'\right]\right\} , \tag{3.5}$$

$$\nu' = \frac{2\mu}{r(1 - 2\mu)} + r\left(1 + \frac{\bar{\psi}\psi}{4\mathfrak{r}^2}\right)^{-2} \bar{\psi}'\psi' + \frac{8\pi G_\star A^4(\psi, \bar{\psi})rP}{1 - 2\mu} \,, \tag{3.6}$$

$$\psi'' = \frac{2\bar{\psi}\psi'^2}{\bar{\psi}\psi + 4\mathfrak{r}^2} - \frac{2(1 - \mu)}{r(1 - 2\mu)}\psi'$$
$$+ \frac{4\pi G_\star A^4(\psi, \bar{\psi})}{1 - 2\mu}\left[(\rho - 3P)\left(1 + \frac{\bar{\psi}\psi}{4\mathfrak{r}^2}\right)\bar{\kappa}(\psi, \bar{\psi}) + r\psi'(\rho - P)\right] , \tag{3.7}$$

$$\omega'' = \left[r\left(1 + \frac{\bar{\psi}\psi}{4\mathfrak{r}^2}\right)^{-2}\bar{\psi}'\psi' - \frac{4}{r}\right]\omega' + \frac{4\pi G_\star A^4(\psi, \bar{\psi})r(\rho c^2 + P)}{1 - 2\mu}\left(\omega' + \frac{4}{r}\omega\right) , \tag{3.8}$$

where primes denote derivatives with respect to the radial coordinate $x^1 = r$. As usual, the system is closed by specifying a barotropic equation of state $P = P(\rho)$.

For the purpose of numerical integration, it is useful to work out series expansions of the functions $\mu(r)$, $\nu(r)$, $P(r)$, $\psi(r)$, and $\omega(r)$ about $r = 0$:

$$\mu(r) = \frac{4\pi G_\star}{3}A_0^4\rho_0 r^2 + \mathcal{O}(r^4) \,, \tag{3.9}$$

$$\nu(r) = \nu_0 + \frac{4\pi G_\star}{3}A_0^4(\rho_0 + 3P_0)r^2 + \mathcal{O}(r^4) \,, \tag{3.10}$$

$$P(r) = P_0 - \frac{2\pi G_\star}{3}A_0^4(\rho_0 + P_0)\left[\rho_0 + 3P_0 + \bar{\kappa}_0\kappa_0\left(\rho_0 - 3P_0\right)\right]r^2 + \mathcal{O}(r^4) \,, \tag{3.11}$$

$$\psi(r) = \psi_0 + \frac{2\pi G_\star}{3}A_0^4\bar{\kappa}_0(\rho_0 - 3P_0)\left(1 + \frac{\bar{\psi}_0\psi_0}{4\mathfrak{r}^2}\right)r^2 + \mathcal{O}(r^4) \,, \tag{3.12}$$

$$\omega(r) = \omega_0 + \frac{8\pi G_\star}{5}\omega_0 A_0^4(\rho_0 + P_0)r^2 + \mathcal{O}(r^4) \,. \tag{3.13}$$

Here the subscript 0 denotes evaluation at the stellar center $r = 0$.

When ψ and $\bar{\psi}$ are constant and $A(\psi, \bar{\psi}) = 1$ the field equations reduce to the standard Tolman-Oppenheimer-Volkoff equations in GR. Indeed, GR solutions are part of the solution spectrum of TMS theories with $\alpha = 0$ in Eq. (2.23), as in the usual single-scalar case [13, 23]. On the other hand, when $\alpha \neq 0$ the scalar field is forced to have a non-trivial profile in the presence of matter ($T \neq 0$).

Furthermore, even when $\alpha = 0$, other solutions characterized by a non-trivial profile for the scalar fields can co-exist with the GR solutions; in Appendix C we give a simple interpretation of these "spontaneously scalarized" solutions in terms of a tachyonic instability of relativistic GR solutions. Besides their gravitational mass M and radius R, scalarized neutron stars are characterized by their scalar charge Q, which is generally a complex number for the complex scalar field ψ discussed here*.

---

* Note that Q is defined in terms of a specific target-space coordinate system. Observable quantities

The gravitational mass M and the scalar charge Q of stellar models in TMS theories can be computed by integration in the vacuum exterior region, where $P = \rho = 0$. We integrate the structure equations outwards from $r = 0$ up to a point $r = R$ such that $P(R) = 0$, which determines the stellar surface in the Einstein frame. The areal radius $\tilde{R}$ in the Jordan frame can be obtained rescaling R by the conformal factor $A(\psi, \bar{\psi})$, which depends on the value of the scalar field ψ and its complex conjugate $\bar{\psi}$ at $r = R$. The values of the mass function m, of the scalar field ψ and of its derivative ψ' at $r = R$ are used as initial conditions to integrate the structure equations in the exterior region. In practice, the integration is terminated at some finite but large grid point where $r = R_\infty$. From the values of m, ψ and ψ' at R_∞ we can determine M and Q by solving the system of equations

$$m(r) = M - \frac{|Q|^2}{2r} - \frac{M|Q|^2}{2r^2} + \mathcal{O}\left(\frac{1}{r^3}\right), \tag{3.14}$$

$$\psi(r) = \psi_\infty + \frac{Q}{r} + \frac{QM}{r^2} + \mathcal{O}\left(\frac{1}{r^3}\right), \tag{3.15}$$

$$\psi'(r) = -\frac{Q}{r^2} + \mathcal{O}\left(\frac{1}{r^3}\right). \tag{3.16}$$

where ψ_∞ is the constant background value of the scalar field. Therefore we have three equations to solve for three unknowns: M, Q and ψ_∞. The physical solution of interest is the one corresponding to the particular central value of the scalar field ψ_0 (which can be found e.g. by a shooting method) such that the background field vanishes, i.e. $\psi_\infty = 0$.

As an alternative integration technique, we have also implemented a compactified coordinate grid in the vacuum exterior introducing a variable $y \equiv 1/r$, which results in a regular set of differential equations that is readily integrated to spatial infinity at $y = 0$. The gravitational mass M, scalar charge Q and asymptotic scalar field magnitude are then directly obtained from $m(y = 0)$, $\psi(y = 0)$ and $\partial_y \psi(y = 0)$, and numerical shooting provides a fast-converging algorithm to enforce the boundary condition $\lim_{y \to 0} \psi = 0$. The two independent integrators yield bulk stellar properties that agree within $\sim 1\%$ or better.

3.2. Numerical integration and results

In this section we discuss the result of the numerical integration of the hydrostatic equilibrium equations in the TMS theory of Section 2.4. Our main interest is to understand scalarization in this model, and for simplicity in this paper we will focus on static stars. We will use the polytropic equation of state labeled "EOS1" in Ref. [30], for which the pressure P and the energy density ρ are given as functions of the baryonic density n_B by

$$P = Kn_0 m_B \left(\frac{n_B}{n_0}\right)^\gamma, \qquad \rho = n_B\, m_B + K\frac{n_0 m_B}{\gamma - 1}\left(\frac{n_B}{n_0}\right)^\gamma, \tag{3.17}$$

where $n_0 = 0.1$ fm^{-3}, $m_B = 1.66 \times 10^{-27}$ kg, $K = 0.0195$ and $\gamma = 2.34$. Therefore, the function $\rho = \rho(P)$ can be constructed parametrically by varying n_B.

---

must be invariant under changes of coordinates, and can thus only depend on target-space scalars such as $|Q|^2$, or $|Q_A - Q_B|^2$ (for a binary system with bodies A and B), or more complicated contractions.

3.2.1.   The $O(2)$-symmetric theory In the absence of a scalar potential, the gravitational part of the action (2.1) is invariant under the target-space isometry group G. For our simple two-real-scalar model with maximally symmetric target space, G is the orthogonal group $O(3)$ in the case of spherical geometry, the indefinite orthogonal group $O(2,1)$ in the case of hyperbolic geometry, and the inhomogeneous orthogonal group $IO(2) = \mathbb{R}^2 \rtimes O(2)$ in the case of flat geometry.

When scalar-matter couplings are introduced, the action is no longer invariant under all of G, but only under some subgroup $H < G$. As a first example, let us consider the particular case in which $\beta_1 = \alpha = 0$. In this case the conformal factor $A(\psi, \bar{\psi})$ given in Eq. (2.24) reduces to

$$A(\psi, \bar{\psi}) = \exp\left(\frac{1}{2}\beta_0 \psi\bar{\psi}\right) , \qquad (3.18)$$

where again we have neglected higher-order terms in the scalar field. This equation is obviously invariant under rotations in the complex plane ($\psi \to \psi\, e^{i\theta}$) and complex conjugation ($\psi \to \bar{\psi}$). Therefore, $H = O(2)$. Note that the boundary condition $\psi_\infty = 0$ is H-invariant. We refer to this special case as the $O(2)$-symmetric TMS theory. In this theory, a GR stellar configuration with $\psi \equiv 0$ is always a solution that is $O(2)$-invariant.

We now construct scalarized solutions, which spontaneously break the $O(2)$ symmetry. They depend on the two real parameters (β_0 and $\mathfrak{r}^2$) of this theory, as well as the central baryon density n_B. The $O(2)$–symmetric character of the scalarized solution space is exhibited in Fig. 3.1, where we show that, for given values of $\mathfrak{r}$ and n_B, there exists an infinite number of scalarized solutions characterized by a different value of the complex field ψ_0 at the center of the star. The different values of the scalar field are related by a phase rotation, and the masses and radii of neutron star models along each of the circles shown in Fig. 3.1 are identical. The target-space curvature $\mathfrak{r}$ has the effect of suppressing ($\mathfrak{r}^2 < 0$) or increasing ($\mathfrak{r}^2 > 0$) the value of $|\psi_0|$, and consequently of the scalar charge Q. Therefore a spherical target space ($\mathfrak{r}^2 > 0$) produces stronger scalarization effects in the mass-radius relations with respect to the case of a flat target-space metric, as illustrated in Fig. 3.2. On the other hand, a hyperbolic target space ($\mathfrak{r}^2 < 0$) tends to reduce the effects of spontaneous scalarization. This can be intuitively, if not rigorously, understood by a glance at Eqs. (2.18) and (2.19): the curvature term plays the role of an "effective (field-dependent) gravitational constant" which is either larger or smaller than the "bare" gravitational constant depending on whether $\mathfrak{r}^2 > 0$ or $\mathfrak{r}^2 < 0$. In both cases, as $\mathfrak{r} \to \infty$ the solution reduces (modulo a trivial phase rotation) to that of a ST theory with a single real scalar field ψ and scalar-matter coupling $A(\psi) = \exp\left(\frac{1}{2}\beta_0 \psi^2\right)$. We remark that due to the $O(2)$ symmetry, all solutions of this theory are equivalent to solutions with $\text{Im}[\psi] = 0$; as discussed in Section 3.2.2 below, these are effectively – modulo a field redefinition – solutions of a single-scalar theory.

Finally, in Fig. 3.3 we illustrate the radial profiles of the mass function m, metric potential ν, mass-energy density ρ and scalar field ψ for scalarized stellar models with fixed baryonic mass $M_B = 1.70\ M_\odot$ in theories with $\beta_0 = -5.0$ and $\mathfrak{r}^2 = \pm 1/4$.

3.2.2. The full TMS theory   We now turn our attention to the existence of scalarized stellar models in the theory defined by Eq. (2.23), which depends on three real parameters (β_0, β_1 and $\mathfrak{r}^2$) and the complex constant α. When $\alpha = 0$ and $\beta_1 \neq 0$,
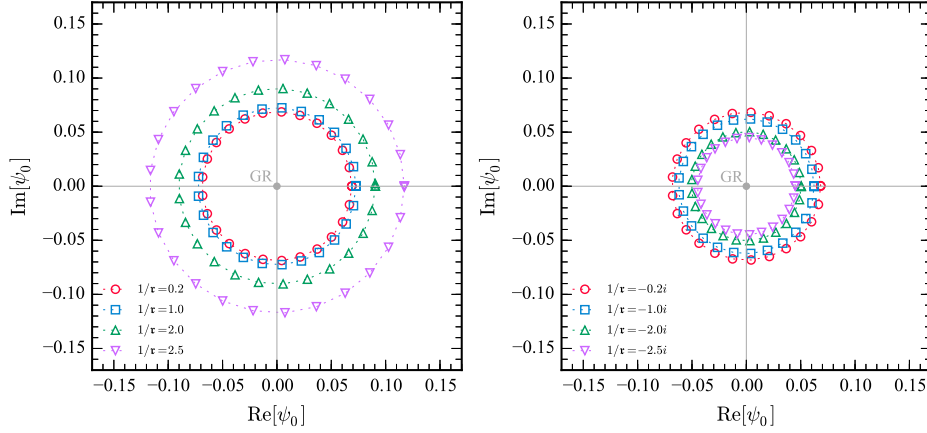
Figure 3.1. *Spontaneous scalarization in a TMS theory with $O(2)$ symmetry.* The value ψ_0 of the scalar field at the center of the star for scalarized solutions in the $O(2)$–symmetric theory with $\beta_0 = -5.0$ and central baryon density $n_B = 10.4\,n_{\text{nuc}}$, where the nuclear density is $n_{\text{nuc}} = 10^{44}\,\text{m}^{-3}$. *Left panel:* spherical target space with $\mathfrak{r}^2 > 0$. *Right panel:* hyperbolic target space with $\mathfrak{r}^2 < 0$. In both panels the origin corresponds to the neutron star solution in GR.
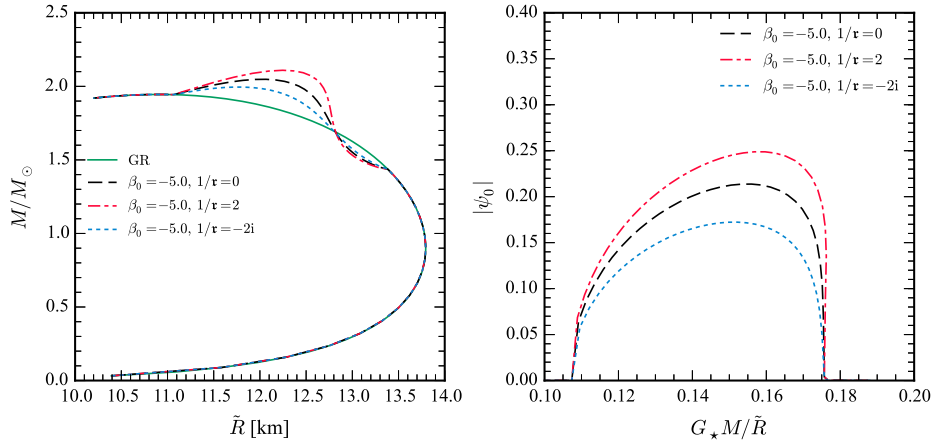

Figure 3.2. *Stellar properties in the $O(2)$–symmetric theory. Left panel:* The mass-radius relation for different values of $\mathfrak{r}$ and $\beta_0 = -5.0$. *Right panel:* Central value of the magnitude of the scalar field $|\psi_0|$ as a function of the stellar compactness $G_\star M/(\tilde{R}c^2)$. Here $\tilde{R}$ is the areal Jordan-frame radius of the star. The onset of scalarization does not depend on the value of $\mathfrak{r}$.

this theory is invariant under the symmetry group $Z_2 \times Z_2$ generated by conjugation $(\psi \to \bar{\psi})$ and inversion $(\psi \to -\psi)$. Introduction of $\alpha \in \mathbb{R}$ partially breaks this symmetry down to Z_2, consisting of conjugation only, whereas introduction of $\alpha \in \mathbb{C} \backslash \mathbb{R}$ fully breaks this symmetry.

An interesting question is whether there exists a region of the parameter space of this theory in which *both* fields scalarize∗. We first searched for such "biscalarized"

─────────────

∗ This question is not invariant under field redefinitions. More precisely, we ask whether there exists a
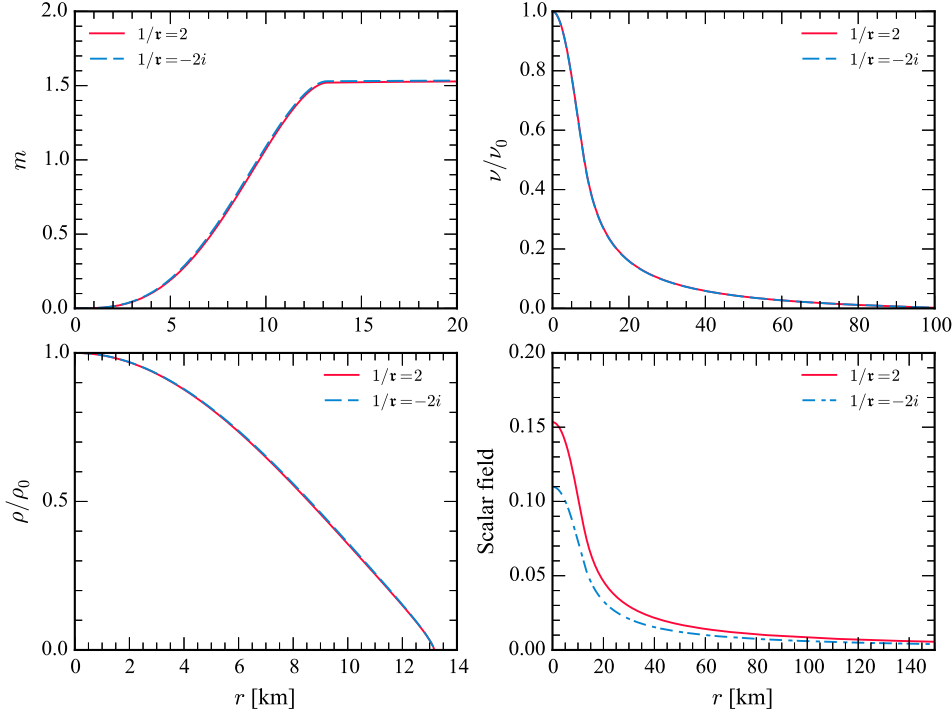
Figure 3.3. *Radial profiles.* Different panels show the profiles of the mass function m, metric potential ν, total energy density ρ and complex scalar field ψ, in units of $c = G = M_\odot = 1$. The profiles correspond to a scalarized star in the $O(2)$-symmetric theory with $\beta_0 = -5.0$, $\beta_1 = \alpha = 0$, and fixed baryon mass $M_B = 1.70\ M_\odot$. The target space curvature is either $\mathfrak{r} = 0.5$ (spherical) or $\mathfrak{r} = 0.5i$ (hyperboloidal). In the spherical case, the scalarized solution has a gravitational mass $M = 1.54\ M_\odot$, Jordan-frame areal radius $\tilde{R} = 13.0$ km, total scalar charge $Q = 0.553\ M_\odot$ and central scalar magnitude $|\psi_0| = 0.154$. In the hyperbolic case, these quantities are $M = 1.54\ M_\odot$, $\tilde{R} = 13.0$ km, $Q = 0.393\ M_\odot$ and $|\psi_0| = 0.110$. For comparison, the GR solution with the same baryonic mass has $M = 1.54\ M_\odot$ and $R = \tilde{R} = 13.2$ km.

solutions in the $Z_2 \times Z_2$ theory with $\alpha = 0$, considering a wide range of the $(\beta_0, \beta_1, \mathfrak{r})$ space, but we could not find any. However, the situation is dramatically different when $\alpha \neq 0$. Crucially, $|\alpha|$ has to be small enough to satisfy the observational bounds summarized in Appendix B, and in particular Eq. (B.3), but $\arg \alpha$ is completely unconstrained by weak-field observations. Our numerical findings are in agreement with an approximate analytical model which will be presented elsewhere [51]. In the following we discuss the cases $\alpha = 0$ and $\alpha \neq 0$ separately.

Case $\alpha = 0$: breaking the $O(2)$ symmetry down to $Z_2 \times Z_2$ When $\alpha = 0$ but $\beta_1 \neq 0$, we found solutions where only *either the real or the imaginary part* of the scalar field has a non-trivial profile. Therefore, in this case the circle shown in Fig. 3.1 for the $O(2)$-symmetric theory collapses down to four discrete points on the real and imaginary axes (cf. Fig. 3.4).

doubly scalarized solution which can not be described by an effective single-real-scalar theory.
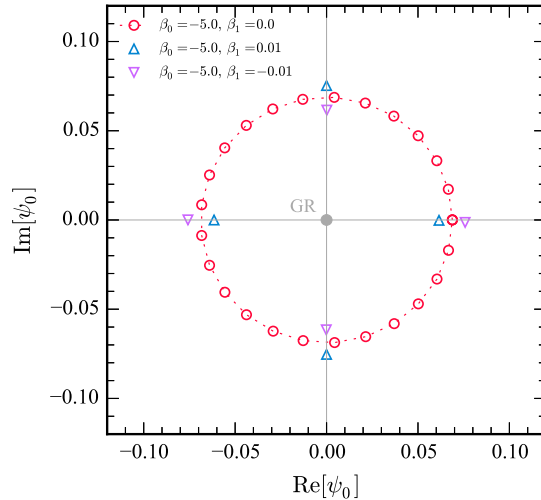
Figure 3.4. *Symmetry breaking of the space of solutions.* When $\beta_1 \neq 0$, the $O(2)$-symmetric solution-space analyzed in the previous section (cf. Fig. 3.1) collapses down to a $(Z_2 \times Z_2)$-symmetric solution-space. This property of the theory is here illustrated for stellar models with the same equation of state and central energy density as in Fig. 3.1, $\beta_0 = -5.0$ and $\mathfrak{r} = 5.0$.

In Appendix C we perform a linear analysis of the field equations, deriving the conditions for scalarization to occur. From Eqs. (C.2), (C.3) and (C.5) we expect that scalarized models exist if $\beta_0 + \beta_1 \lesssim -4.35$ when $\text{Re}[\psi] \neq 0$, or $\beta_0 - \beta_1 \lesssim -4.35$ when instead $\text{Im}[\psi] \neq 0$. We have checked this expectation by calculating models for the parameter sets (i) $1/\mathfrak{r} = 0$, $\beta_1 = 0$ and (ii) $1/\mathfrak{r} = 2$, $\beta_1 = 0$. For each of these cases, we have varied the central density from 10^{-5} km^{-2} to 0.0015 km^{-2} in steps of 10^{-5} km^{-2}. We applied our shooting algorithm for a scalar field amplitude $|\psi(r = 0)| \in [0, 1]$ in steps of 0.1, choosing discrete values of the complex phase $\theta = 0$, $\pi/2$, π, $3\pi/2$, and varying $\beta_0 \in [-20, 3]$ in steps of 0.01. For all values of the central density and β_0, the shooting method identifies one GR solution model with vanishing scalar charge. For sufficiently negative β_0, we additionally identify scalarized models. Among these models we then identify for a given value of β_0 the scalarized model with the lowest baryon mass, and thus generate a scalarization plot analogous to Fig. 2 in [46] for ST theory with a single scalar field. The result is shown in Fig. 3.5. The small difference between the curves for different curvature radius $\mathfrak{r}$ likely arises from the small but finite amplitude of the scalar field appearing in the lowest-mass scalarized binaries, which is a byproduct of finite discretization in the mass parameter space. In the continuum limit of infinitesimal amplitudes of the scalar field in scalarized models, we expect this difference to disappear completely and the dotted and dashed curves to overlap. This is indeed supported by an analytic calculation.∗ These results confirm the prediction of Eq. (C.5) and agree (qualitatively and quantitatively) with the single-scalar case shown in Fig. 2 of [46].

∗ This calculation uses Riemann-normal coordinates at φ_∞ in target space, and finds that target-space-curvature terms appear in the field equations at third order in the scalar-amplitude expansion. Details will be published elsewhere [51].
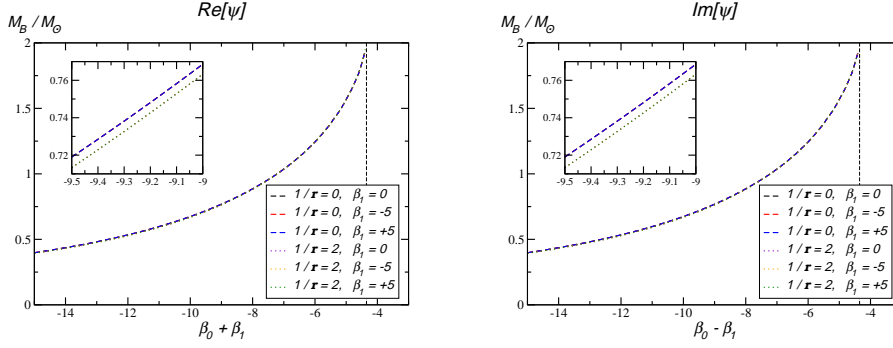
Figure 3.5. *Minimal baryonic mass of scalarized models.* The baryon mass of scalarized solutions at the onset of scalarization as a function of (i) $\beta_0 + \beta_1$ for models where $\mathrm{Re}[\psi]$ is non-zero (left panel) and (ii) $\beta_0 - \beta_1$ for models where $\mathrm{Im}[\psi]$ is non-zero (right panel). Each panel contains 6 curves, corresponding to the three values of β_1 at fixed $\mathfrak{r} = \infty$ (dashed curves) and the same three values of β_1 at $\mathfrak{r} = 1/2$ (dotted curves). The three dashed curves and the three dotted curves, respectively, are indistinguishable in the plot and the two families of dashed and dotted curves are only distinguishable in the inset, where we zoom into a smaller region. In both panels, the vertical long-dashed curve denotes the value $\beta_0 \pm \beta_1 = -4.35$ above which we no longer identify scalarized models, in agreement with Eq. (C.5). From Eq. (2.25) it is clear that the natural parameters are $\beta_0 + \beta_1$ and $\beta_0 - \beta_1$ when the theory is written in terms of the real and imaginary part of ψ, respectively.

Indeed, in this case the analogy with the single-scalar case can be made more formal. Let us consider without loss of generality the subspace of the solution space in which the scalar field is real, i.e. $Z = \mathrm{Re}[\psi] \neq 0$, $W = \mathrm{Im}[\psi] = 0$. The kinetic term can be put in the canonical form by a scalar field redefinition, i.e.

$$K = -\frac{1}{2}\left(1 + \frac{Z^2}{4\mathfrak{r}^2}\right)^{-2} \partial_\mu Z \partial^\mu Z = -\frac{1}{2}\partial_\mu \tilde{Z} \partial^\mu \tilde{Z}\,, \qquad (3.19)$$

where the two fields are related by $Z = 2\mathfrak{r}\tan\left(\frac{\tilde{Z}}{2\mathfrak{r}}\right)$, and $-\pi\mathfrak{r} < \tilde{Z} < \pi\mathfrak{r}$. For $|Z| \ll \mathfrak{r}$ we have

$$\tilde{Z} = Z - \frac{Z^3}{12\mathfrak{r}^2} + O(Z^5)\,, \qquad Z = \tilde{Z} + \frac{\tilde{Z}^3}{12\mathfrak{r}^2} + O(\tilde{Z}^5)\,. \qquad (3.20)$$

Replacing this Taylor expansion in the conformal factor (2.24) we see that the parameters β_0, β_1 remain the same. In particular, we obtain $A(\tilde{Z}) = \exp\left[(\beta_0 + \beta_1)\tilde{Z}^2/2\right]$ (plus higher-order terms), i.e., the coupling function coincides with that of a single-scalar theory with coupling constant $\beta = \beta_0 + \beta_1$. Thus, as long as $|Z| \ll \mathfrak{r}$, the theory with $\alpha = 0$ is equivalent to a ST theory with one scalar and coupling $\beta = \beta_0 + \beta_1$ (or $\beta = \beta_0 - \beta_1$, in which case only $W = \mathrm{Im}[\psi]$ scalarizes). Clearly, this proof also includes the limit $\mathfrak{r} \to \infty$, where the solutions reduce exactly to those of a single-scalar theory with the identification $\beta \equiv \beta_0 + \beta_1$.

When the condition $|Z| \ll \mathfrak{r}$ is not fulfilled, the theory is still equivalent to a ST theory with one scalar field, but the form of the conformal factor A changes. These theories only differ by higher-order terms in the series expansion (2.20), (2.22), which are negligible at the onset of the scalarization.

In Fig. 3.6 we show the mass-radius relation of scalarized neutron star solutions in the non-$O(2)$ symmetric theory for different values of $\mathfrak{r}$ and $\beta_0 + \beta_1$. When the
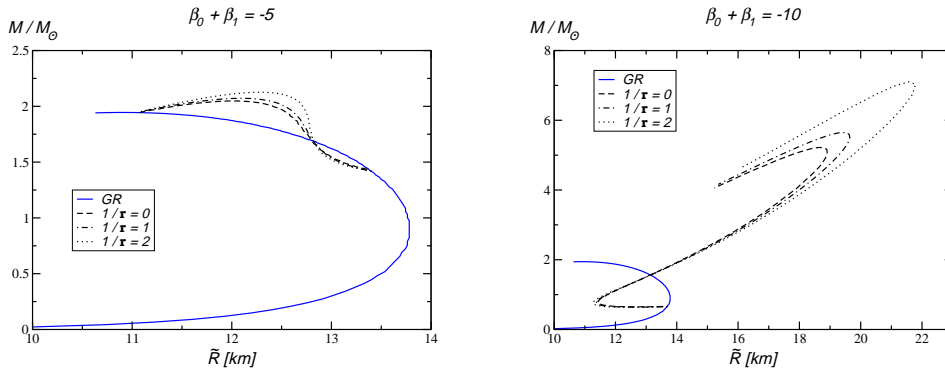
Figure 3.6. *Mass-radius relations in the full TMS theory.* Analogous to the left panel of Fig. 3.2 for three values of the curvature radius of the target metric ($\mathfrak{r} = \infty$, $\mathfrak{r} = 1$ and $\mathfrak{r} = 0.5$), $\beta_0 + \beta_1 = -5$ (left panel) and $\beta_0 + \beta_1 = -10$ (right panel). Here we only consider models where $\mathrm{Re}[\tilde{\psi}] \neq 0$. The gravitational mass M is shown as a function of the Jordan-frame radius $\tilde{R}$. For comparison, we include in both panels the GR curve. Note the different axis ranges in the two panels. When $\mathfrak{r} \to \infty$, the theory reduces to a ST theory with one scalar and effective coupling $\beta = \beta_0 + \beta_1$, and the observational constraint $\beta_0 + \beta_1 \gtrsim -4.5$ is in place [24]. However, such lower bound might be less stringent when $\mathfrak{r}$ is finite.

coupling is large, we observe that the solutions can differ dramatically from their GR counterpart.

Case $\alpha \neq 0$: multi-scalarization   When $\alpha \neq 0$, GR configurations are not solutions of the field equations. In particular, a constant (or vanishing) scalar field does not satisfy Eq. (2.18) when $T \neq 0$. Therefore it is not surprising that when $\alpha \neq 0$ we can find solutions with two non-trivial scalar profiles even when $\beta_0 = \beta_1 = 0$. A more interesting question is whether there are stellar configurations in which both scalar fields have a large amplitude. As we have seen, these "biscalarized" solutions are absent in the $\alpha = 0$ case. Here we present preliminary results that demonstrate the existence of interesting biscalarized solutions as long as $\alpha \neq 0$.

For concreteness we set $|\alpha| = 10^{-3}$: such a small value of $|\alpha|$ satisfies the experimental bounds discussed in Appendix B (but we have also studied the case where $|\alpha| = 10^{-4}$, with qualitatively similar results).

In this preliminary study we vary $\arg \alpha$ in the range $[0, 2\pi]$ in steps of $\pi/6$ and we set $1/\mathfrak{r} = 0$ (i.e., we consider a flat target space). A finite target-space curvature $\mathfrak{r}$ does not change the picture qualitatively; a more detailed analysis will be presented elsewhere [51]. Our search yields several models with non-zero scalar field, as shown in Figs. 3.7 and 3.8, where dots denote the real and imaginary parts of the central value of the scalar field ψ_0 for which solutions were found.

For the time being, we wish to remark two very interesting (and perhaps unexpected) features of these biscalarized solutions:

1) Figure 3.7 shows that the solutions are at least approximately $O(2)$ symmetric when $\beta_1 \sim |\alpha|$, and the $O(2)$ symmetry is broken (the solution "circles" turn into "crosses") when $\beta_1 \gg |\alpha|$. The cross-like shape of the scalarized solutions in the $\mathrm{Re}[\psi_0]$, $\mathrm{Im}[\psi_0]$ plane collapses towards a set of solutions on the vertical line $\mathrm{Re}[\psi_0] = 0$ for the larger values of β_1 (bottom panels in Fig. 3.7). This behavior
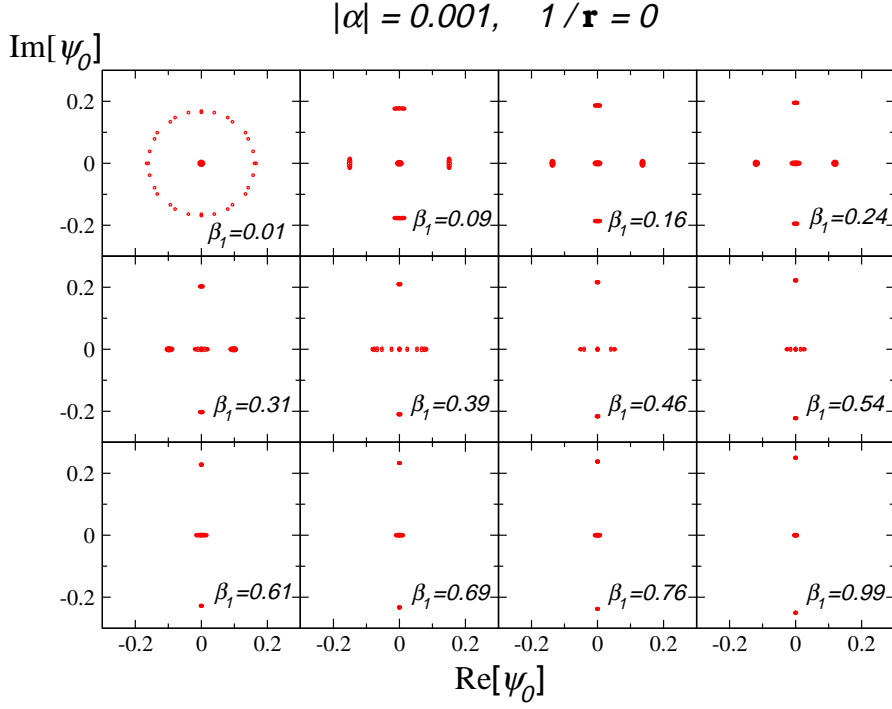
Figure 3.7. *Scalar field amplitudes in the full TMS theory - I.* Scalar field amplitude at the stellar center ψ_0 for stellar models with $\beta_0 = -5$, $|\alpha| = 0.001$ and fixed baryon mass $M_B = 1.8 \, M_\odot$. The different panels show the solutions found for different values of β_1 as indicated in each panel. In each case, we vary the phase of α from 0 to 2π in steps of $\pi/6$. In contrast to the $\alpha = 0$ case in Fig. 3.4, the breaking of the $O(2)$ symmetry occurs gradually as β_1 is increased away from 0.

can be interpreted as an approximation to the spontaneous scalarization for the case $\alpha = 0$ displayed in Fig. 3.5, and discussed in the text around Eqs. (3.19) and (3.20). There we observed that spontaneous scalarization of $\mathrm{Re}[\psi]$ occurs (in analogy with the single-field case) if $\beta_0 + \beta_1 \lesssim -4.35$, and scalarized models with a large imaginary part $\mathrm{Im}[\psi]$ exist if $\beta_0 - \beta_1 \lesssim -4.35$. The biscalarized models in Fig. 3.5 have been calculated for fixed $\beta_0 = -5$. For $\beta_1 \gtrsim 0.65$ we therefore enter the regime where $\beta_0 + \beta_1 \gtrsim -4.35$, and we no longer expect to find models with strongly scalarized $\mathrm{Re}[\psi]$. The condition $\beta_0 - \beta_1 \lesssim -4.35$ for scalarization of $\mathrm{Im}[\psi]$, however, remains satisfied, so that scalarized models should cluster close to the $\mathrm{Re}[\psi_0]$–axis. This is indeed observed in the bottom panels of Fig. 3.7. Note that in this case the condition $\beta_1 \gtrsim 0.65 \gg |\alpha| = 10^{-3}$ is satisfied, in close correspondence to the case $\alpha = 0$ of Fig. 3.5.

2) Figure 3.8 (which is a "zoom-in" on the top-left panel of Figure 3.7) indicates additional fine structure in the space of solutions, with at least three different families of scalarized solutions having remarkably different values of the scalar field (and therefore of the scalar charge).
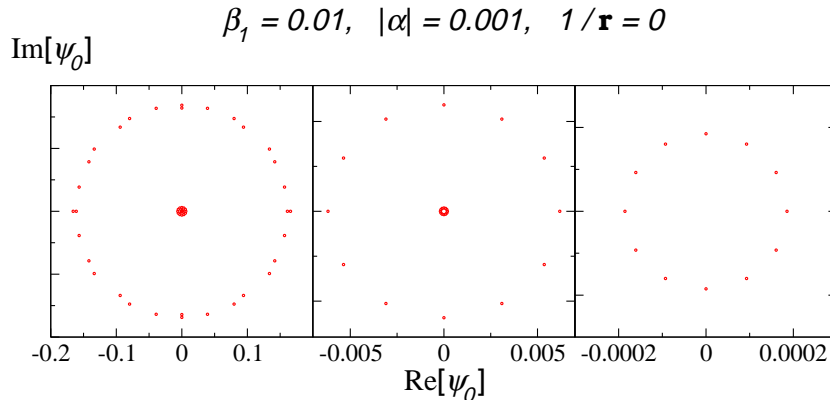
Figure 3.8. *Scalar field amplitudes in the full TMS theory - II.* The data of the upper left panel of Fig. 3.7 are shown on different scales to resolve the fine structure of the solutions in the ψ_0 plane. In each panel the vertical extent is equal to the horizontal.

When $\mathbf{r} \to \infty$, binary pulsar observations in the single-scalar case would impose a constraint equivalent to $\beta_0 + \beta_1 \gtrsim -4.5$ [24]. More work is required to clarify whether a similar constraint is in place also for multiple scalars. Preliminary calculations indicate that the target-space curvature should affect the energy flux from compact binaries at high post-Newtonian order. However, it is unclear whether the formalism of [13] for describing orbital binary dynamics is applicable to the theory studied in this paper, due to the discontinuity at $\alpha = 0$. Furthermore, for multiple scalars, it is possible that some combination of β_0 and β_1 other than their sum may be constrained by binary pulsar observations. A detailed answer to this question requires two theoretical developments that are currently missing: (1) the investigation of stellar structure in generic TMS theories to understand the effect of the theory parameters on stellar properties, and (2) an implementation of these stellar structure calculations in flux formulas similar to those derived in [13] (or generalizations thereof). These are important tasks that should be addressed in future work. In Fig. 3.6 we adopt an agnostic point of view and use large values of $\beta_0 + \beta_1$ in order to illustrate the effect of scalarization in TMS theory in some extreme cases. The phenomenological implications and the stability of biscalarized stellar models will be discussed elsewhere [51].

4. 3+1 formulation of the field equations for numerical relativity

Studies of the strong-field dynamics of compact stars and black holes, whether isolated or in binary systems, require the fully non-linear theory without any symmetry assumptions. Such studies can now be carried out using numerical relativity techniques, and they have already led to new insights into the behavior of ST theories. For example, numerical simulations of neutron star binaries in single-scalar theories have identified a new phenomenon ("dynamical scalarization") occurring in the late stages of the inspiral, just before merger [25, 27, 52]. Similarly, studies of equilibrium sequences of neutron star binaries have shown that dynamical scalarization can lead to a reduction of the number of gravitational-wave cycles with respect to GR [29]. Scalar radiation has also been identified in the inspiral of black hole binaries when the

binary is embedded in a non-trivial scalar background gradient [44,45]. All numerical studies rely on a formulation of the theory suitable for numerical implementation, which is most commonly achieved in terms of a space-time (or 3+1) decomposition of the field equations. Here we present the 3+1 formulation of the field equations for general multi-scalar theories. The work presented in this section is a prerequisite for future numerical studies of multi-scalar theories, and we hope that it will motivate other researchers to investigate this interesting, unexplored topic.

4.1. Action, stress-energy tensor and field equations

We consider a multi-scalar theory described by the action (2.1):

$$S = \frac{1}{4\pi G_\star} \int d^4x \sqrt{-g} \left[\frac{R}{4} - \frac{1}{2} g^{\mu\nu} \gamma_{AB}(\varphi) \partial_\mu \varphi^A \partial_\nu \varphi^B - V(\varphi) \right] + S_{\rm m}[A^2(\varphi)g_{\mu\nu}; \Psi] \,. \tag{4.1}$$

For computational purposes it is useful to consider the scalar fields themselves as ordinary matter, described by the stress-energy tensor $T^{(\varphi)}_{\mu\nu}$ defined in Eq. (2.7):

$$8\pi G_\star T^{(\varphi)}_{\mu\nu} = 2\gamma_{AB} \left(\partial_\mu \varphi^A \partial_\nu \varphi^B - \frac{1}{2} g_{\mu\nu} g^{\alpha\beta} \partial_\alpha \varphi^A \partial_\beta \varphi^B \right) - 2g_{\mu\nu} V \,, \tag{4.2}$$

while $T_{\mu\nu}$, defined in Eq. (2.4), is associated to the fields Ψ (for instance, the fluid composing a neutron star). The total stress-energy tensor, then, is $T_{\mu\nu} + T^{(\varphi)}_{\mu\nu}$. This allows us to use the $3+1$ decomposition of Einstein's equations given in [53], with the replacement $T_{\mu\nu} \to T_{\mu\nu} + T^{(\varphi)}_{\mu\nu}$. Since

$$\begin{aligned} \frac{16\pi G_\star}{\sqrt{-g}} \frac{\delta S}{\delta g^{\mu\nu}} =& R_{\mu\nu} - 2\gamma_{AB}\partial_\mu \varphi^A \partial_\nu \varphi^B - \frac{1}{2} g_{\mu\nu} \left(R - 2\gamma_{AB} g^{\alpha\beta} \partial_\alpha \varphi^A \partial_\beta \varphi^B - 4V \right) \\ & - 8\pi G_\star T_{\mu\nu} = 0 \,, \end{aligned} \tag{4.3}$$

Einstein's equations have the form $R_{\mu\nu} - (1/2)g_{\mu\nu}R = 8\pi G_\star(T_{\mu\nu} + T^{(\varphi)}_{\mu\nu})$. The trace of Eq. (4.3) yields

$$-R + 2\gamma_{AB} g^{\alpha\beta} \partial_\alpha \varphi^A \partial_\beta \varphi^B + 8V - 8\pi G_\star T = 0 \,, \tag{4.4}$$

where $T = g^{\mu\nu} T_{\mu\nu}$, and therefore we have

$$R_{\mu\nu} - 2\gamma_{AB}\partial_\mu \varphi^A \partial_\nu \varphi^B - 2g_{\mu\nu}V - 8\pi G_\star \left(T_{\mu\nu} - \frac{1}{2} g_{\mu\nu} T \right) = 0 \,. \tag{4.5}$$

By varying the action (4.1) with respect to φ^A one gets the scalar field equation

$$\begin{aligned} 4\pi G_\star \frac{\gamma^{AB}}{\sqrt{-g}} \frac{\delta S}{\delta \varphi^B} =& \Box \varphi^A + \gamma^A_{CD} g^{\mu\nu} \partial_\mu \varphi^C \partial_\nu \varphi^D - \gamma^{AB} \frac{\partial V}{\partial \varphi^B} \\ & + 4\pi G_\star \gamma^{AB} \frac{\partial \log A}{\partial \varphi^B} T = 0 \,, \end{aligned} \tag{4.6}$$

where γ^A_{CD} are the Christoffel symbols on the target space.

4.2. 3 + 1 decomposition

As discussed in Ref. [45] (see also [53]), we consider a slicing of the spacetime in a set of surfaces Σ. We introduce the normal n_μ to those surfaces and the projector

$$h_{\mu\nu} = g_{\mu\nu} + n_\mu n_\nu \,, \tag{4.7}$$

and write the metric in the form ($\mu, \nu = 0, \ldots, 3$; $i, j = 1, 2, 3$)

$$ds^2 = g_{\mu\nu} dx^\mu dx^\nu = -\alpha^2 dt^2 + h_{ij}(dx^i + \beta^i dt)(dx^j + \beta^j dt) \,, \tag{4.8}$$

where α, β^i and h_{ij} are the lapse, the shift, and the metric on Σ, respectively. We remark that in these coordinates $n_i = 0$, therefore the 3-dimensional metric coincides with the projector (4.7) restricted to the spatial indices. It is also worth noting that $h^{0\mu} = 0$, and $g^{\mu\nu} h_{\mu\nu} = 3$.

We define the covariant derivative on Σ as $D_i \equiv h_i{}^\alpha \nabla_\alpha$. Since $\partial_t = \alpha n + \beta$, the Lie derivative with respect to n is $\mathcal{L}_n = (\partial_t - \mathcal{L}_\beta)/\alpha$. The extrinsic curvature is defined as

$$K_{\mu\nu} \equiv -h_\mu{}^\sigma \nabla_\sigma n_\nu \,. \tag{4.9}$$

Its contravariant form is purely spatial, i.e., $K^{0\mu} = 0$. The extrinsic curvature satisfies the relation $K_{ij} = \mathcal{L}_n h_{ij}/2$, so the evolution equation for the metric reads

$$\mathcal{L}_n h_{ij} = -2K_{ij} \,. \tag{4.10}$$

Other useful relations are [53, 54]

$$\nabla^\mu n_\mu = -K \,, \quad n^\mu \nabla_\mu n^\nu = D^\nu(\ln \alpha) \,, \tag{4.11}$$

where we defined $K \equiv g_{\mu\nu} K^{\mu\nu}$.

In the same way, we can define the curvature of each of the scalar fields as $K_\varphi^A \equiv -\mathcal{L}_n \varphi^A/2$. Consequently, the evolution equation for the scalar fields reads

$$\mathcal{L}_n \varphi^A = -2K_\varphi^A \,, \tag{4.12}$$

where we note that $\mathcal{L}_n \varphi^A = n^\mu \varphi_\mu^A$.

It will also be useful to decompose the quantity $g^{\alpha\beta} \partial_\alpha \varphi^A \partial_\beta \varphi^B$ as follows:

$$g^{\alpha\beta} \partial_\alpha \varphi^A \partial_\beta \varphi^B = (h^{\alpha\beta} - n^\alpha n^\beta) \partial_\alpha \varphi^A \partial_\beta \varphi^B = D^i \varphi^A D_i \varphi^B - 4K_\varphi^A K_\varphi^B \,. \tag{4.13}$$

4.2.1. Einstein's equations The $3 + 1$ decomposition of Einstein's equations with matter is given e.g. in Eqs. (2.4.6), (2.4.9) and (2.5.6) of [53]; in those equations the matter terms are expressed in terms of the quantities $\rho = n^\mu n^\nu T_{\mu\nu}$, $j^i = -h^{i\mu} n^\nu T_{\mu\nu}$, and $S_{ij} = h_i{}^\alpha h_j{}^\beta T_{\alpha\beta}$. We simply replace in those equations $T_{\mu\nu} \to T_{\mu\nu} + T_{\mu\nu}^{(\varphi)}$, where the explicit expression of $T_{\mu\nu}^{(\varphi)}$ is given in Eq. (4.2), i.e., we replace $\rho \to \rho + \rho^{(\varphi)}$, $j^i \to j^i + j^{i(\varphi)}$, $S_{ij} \to S_{ij} + S_{ij}^{(\varphi)}$, where:

$$8\pi G_\star \rho^{(\varphi)} = \gamma_{AB} \left[D^i \varphi^A D_i \varphi^B + 4K_\varphi^A K_\varphi^B \right] + 2V \,, \tag{4.14}$$

$$8\pi G_\star j^{i(\varphi)} = -2\gamma_{AB} D^i \varphi^A(-2K_\varphi^B) = 4\gamma_{AB} D^i \varphi^A K_\varphi^B \,, \tag{4.15}$$

$$8\pi G_\star S_{ij}^{(\varphi)} = 2\gamma_{AB} \left[D_i \varphi^A D_j \varphi^B + 2h_{ij} K_\varphi^A K_\varphi^B - \frac{1}{2} h_{ij} D_i \varphi^A D^i \varphi^B \right] - 2h_{ij} V \,. \tag{4.16}$$

We also have:

$$4\pi G_\star \left[(S^{(\varphi)} - \rho^{(\varphi)})h_{ij} - 2S_{ij}^{(\varphi)} \right] = -2\gamma_{AB}D_i\varphi^A D_j\varphi^B - 2h_{ij}V \, . \tag{4.17}$$

Then Eqs. (2.4.6), (2.4.9) and (2.5.6) of [53] give:

$$
\begin{aligned}
^{(3)}R + K^2 - K_{\mu\nu}K^{\mu\nu} &= 16\pi G_\star \rho, \\
&\quad + 2\gamma_{AB}\left[D^i\varphi^A D_i\varphi^B + 4K_\varphi^A K_\varphi^B\right] + 4V,
\end{aligned}
\tag{4.18}
$$

$$D_j(K^{ij} - h^{ij}K) = 8\pi G_\star j^i + 4\gamma_{AB}D^i\varphi^A K_\varphi^B \tag{4.19}$$

and

$$
\begin{aligned}
\mathcal{L}_n K_{ij} = &- D_i D_j(\ln\alpha) + \, ^{(3)}R_{ij} + KK_{ij} - 2K_{ik}K^k_{\ j} + 4\pi G_\star \left[h_{ij}(S - \rho) - 2S_{ij}\right] \\
&- 2\gamma_{AB}D_i\varphi^A D_j\varphi^B - 2h_{ij}V \, ,
\end{aligned}
\tag{4.20}
$$

where $^{(3)}R_{ij}$ and $^{(3)}R$ are the Ricci tensor and the Ricci scalar of the metric h_{ij}, respectively.

4.2.2. Scalar field equation   To decompose the scalar equation (4.6), i.e.

$$\Box\varphi^A + \gamma_{CD}^A g^{\mu\nu}\partial_\mu\varphi^C \partial_\nu\varphi^D - \gamma^{AB}\frac{\partial V}{\partial\varphi^B} + 4\pi G_\star \gamma^{AB}\frac{\partial\log A}{\partial\varphi^B}T = 0, \tag{4.21}$$

we start by considering the first term, $\Box\varphi^A$ (the single-scalar case was discussed in [54, 55]). We have:

$$
\begin{aligned}
\Box\varphi^A &= \nabla_\sigma(g^{\sigma\rho}\nabla_\rho\varphi^A) \\
&= \nabla_\sigma\left[(-n^\sigma n^\rho + h^{\sigma\rho})\nabla_\rho\varphi^A\right] = \nabla_\sigma[2n^\sigma K_\varphi^a + D^\sigma\varphi^A] \\
&= 2\mathcal{L}_n K_\varphi^A - 2KK_\varphi^A + D_i D^i\varphi^A + D_\rho(\ln\alpha)D^\rho\varphi^A \, .
\end{aligned}
\tag{4.22}
$$

Then, since $T = S - \rho$, the scalar field equation takes the form

$$
\begin{aligned}
\mathcal{L}_n K_\varphi^A = &\ KK_\varphi^A - \frac{1}{2}D_i D^i\varphi^A - \frac{1}{2}D^i\varphi^A D_i(\ln\alpha) \\
&- \frac{1}{2}\gamma_{CD}^A\left(D^i\varphi^C D_i\varphi^D - 4K_\varphi^C K_\varphi^D\right) + \frac{1}{2}\gamma^{AB}\frac{\partial V}{\partial\varphi^B} \\
&- 2\pi G_\star \gamma^{AB}\frac{\partial\log A}{\partial\varphi^B}(S - \rho) \, .
\end{aligned}
\tag{4.23}
$$

4.3. $3+1$ equations for 2-sphere and 2-hyperboloid

Let us now specialize to scalar fields living in a two-dimensional target space with maximal symmetry and positive or negative curvature, i.e. a sphere or hyperboloid. For simplicity we also assume a vanishing potential ($V \equiv 0$). As discussed in Appendix A, the sphere and hyperboloid are both described in stereographic coordinates by the metric

$$\gamma_{AB} = F\begin{pmatrix} 1 & 0 \\ 0 & 1 \end{pmatrix}, \tag{4.24}$$

with

$$F(Z, W) \equiv \frac{\mathfrak{r}^4}{\left[(Z^2 + W^2)/4 + \mathfrak{r}^2\right]^2} \, . \tag{4.25}$$

Here $\varphi^A = (Z, W)$, and $\mathfrak{r}^2$ is positive (negative) for the sphere (hyperboloid). The Christoffel symbols (see Appendix A) are

$$\gamma^Z_{AB} = \frac{1}{Z^2 + W^2 + \mathfrak{r}^2} \begin{pmatrix} -2Z & -2W \\ -2W & 2Z \end{pmatrix}, \quad \gamma^W_{AB} = \frac{1}{Z^2 + W^2 + \mathfrak{r}^2} \begin{pmatrix} 2W & -2Z \\ -2Z & -2W \end{pmatrix},$$

and Einstein's equations can be written as

$$
\begin{aligned}
{}^{(3)}R + K^2 - K_{\mu\nu}K^{\mu\nu} &= 2\gamma_{AB}\left[D^i\varphi^A D_i\varphi^B + 4K^A_\varphi K^B_\varphi\right] + 16\pi G_\star\rho \\
&= 2F\left[D^i Z D_i Z + D^i W D_i W + 4(K^2_Z + K^2_W)\right] + 16\pi G_\star\rho \, ,
\end{aligned}
\tag{4.26}
$$

$$
\begin{aligned}
D_j(K^{ij} - h^{ij}K) &= 4\gamma_{AB}D^i\varphi^A K^B_\varphi + 8\pi G_\star j^i \\
&= 4F(D^i Z K_Z + D^i W K_W) + 8\pi G_\star j^i \, ,
\end{aligned}
\tag{4.27}
$$

$$
\begin{aligned}
\mathcal{L}_n K_{ij} &= -D_i D_j(\ln\alpha) + {}^{(3)}R_{ij} + KK_{ij} - 2K_{ik}K^k_{j} \\
&\quad - 2\gamma_{AB}D_i\varphi^A D_j\varphi^B + 4\pi G_\star\left[h_{ij}(S - \rho) - 2S_{ij}\right] \\
&= -D_i D_j(\ln\alpha) + {}^{(3)}R_{ij} + KK_{ij} - 2K_{ik}K^k_{j} \\
&\quad - 2F(D_i Z D_j Z + D_i W D_j W) + 4\pi G_\star\left[h_{ij}(S - \rho) - 2S_{ij}\right] \, .
\end{aligned}
\tag{4.28}
$$

Finally, the scalar field equations are

$$
\begin{aligned}
\mathcal{L}_n K_Z &= KK_Z - \frac{1}{2}D_i D^i Z - \frac{1}{2}D^i Z D_i(\ln\alpha) - \frac{1}{2}\gamma^Z_{CD}(D^i\varphi^C D_i\varphi^D - 4K^C_\varphi K^D_\varphi) \\
&= KK_Z - \frac{1}{2}D_i D^i Z - \frac{1}{2}D^i Z D_i(\ln\alpha) + \frac{1}{Z^2 + W^2 + \mathfrak{r}^2} \\
&\quad \times \left[\left(Z D_i Z D^i Z - Z D_i W D^i W + 2W D_i Z D^i W\right)\right. \\
&\quad \left. -4\left(Z K^2_Z - Z K^2_W + 2W K_Z K_W\right)\right] - 2\pi G_\star F^{-1}\frac{\partial\log A}{\partial Z}(S - \rho) \, ,
\end{aligned}
\tag{4.29}
$$

$$
\begin{aligned}
\mathcal{L}_n K_W &= KK_W - \frac{1}{2}D_i D^i W - \frac{1}{2}D^i W D_i(\ln\alpha) - \frac{1}{2}\gamma^W_{CD}(D^i\varphi^C D_i\varphi^D - 4K^C_\varphi K^D_\varphi) \\
&= KK_W - \frac{1}{2}D_i D^i W - \frac{1}{2}D^i W D_i(\ln\alpha) + \frac{1}{Z^2 + W^2 + \mathfrak{r}^2} \\
&\quad \times \left[\left(-W D_i Z D^i Z + W D_i W D^i W + 2Z D_i Z D^i W\right)\right. \\
&\quad \left. -4\left(-W K^2_Z + W K^2_W + 2Z K_Z K_W\right)\right] - 2\pi G_\star F^{-1}\frac{\partial\log A}{\partial W}(S - \rho) \, ,
\end{aligned}
\tag{4.30}
$$

$$\tag{4.31}$$

where we used the expressions of the Christoffel symbols given in Appendix A.

5. Discussion and conclusions

In this paper we have barely scratched the surface of the potentially rich phenomenology of gravitational theories with multiple scalar fields. Several important

issues should be addressed in follow-up work. First of all, it is important to compute experimental bounds on the parameters β_0, $|\beta_1|$, $\mathfrak{r}$, $|\alpha|$ and $\arg\alpha - \frac{1}{2}\arg\beta_1$ that follow from binary pulsar timing [1, 24]. The quadrupole-order scalar and tensor radiation in TMS theories was computed in [13], but it is unclear whether the formalism of [13] is applicable to the theories that we have studied due to the discontinuity at $|\alpha| = 0$. In any case, drawing exclusion diagrams in the multidimensional phase space of the theory would require extensive stellar-structure calculations, that will be presented in future work. Preliminary results suggest that the target-space curvature radius $\mathfrak{r}$ enters the gravitational-wave flux (at least formally) at high post-Newtonian order, and therefore it is quite likely that $\mathfrak{r}$ will be poorly constrained by binary pulsars. This opens the possibility of interesting new phenomenology in the sensitivity window of advanced Earth-based gravitational-wave detectors. Furthermore, it is unclear whether binary pulsar observations will constrain β_0, $|\beta_1|$, or some combination thereof, and the parameter $\arg\alpha - \frac{1}{2}\arg\beta_1$ (which according to our preliminary results plays a crucial role in "biscalarization") is presently unconstrained.

In this work we have mainly presented various formal developments, but also some new physical results, which in our opinion are representative of the behavior of a wide class of TMS theories:

(i) In theories with $\alpha = 0$, GR solutions co-exist with scalarized solutions but (besides the case of $O(2)$-symmetric theories with $\beta_1 = 0$) we could not find any "biscalarized" solution for any value of β_0. In other words, in this case either the real or the imaginary part of the complex scalar field scalarizes but not both, and the $O(2)$ symmetry of the $\beta_1 = 0$ case is broken.

(ii) The $\alpha \neq 0$ case is dramatically different. In this case – even when $|\alpha|$ is small enough to be compatible with Solar System constraints – biscalarized solutions exist, and their existence depends quite critically on the value of $\arg\alpha - \frac{1}{2}\arg\beta_1$. These solutions seem to exist quite generically in the complex-α plane, but their properties strongly depend on the values of β_0 and $|\beta_1|$.

These results were obtained through extensive numerical searches. However, given the large dimensionality of the parameter space, we cannot exclude the existence of other solutions which were not found in our initial searches. An approximate analytical model which supports our results and a more detailed analysis of biscalarization will be presented elsewhere [51].

Some obvious extensions of the present results concern the study of rotating neutron stars in TMS theory (generalizing [46, 56–58]) and of the universal relations valid for neutron stars in general relativity [59, 60], which may or may not hold in this theory. Another possible extension is to relax the assumption of a vanishing potential in the action, i.e. to consider the multi-scalar generalization of massive Brans-Dicke theory [61, 62], and investigate the effect of the scalar field masses on the structure of scalarized neutron stars. The use of more realistic equations of state is pivotal in confronting TMS theory predictions on the evolution of binary pulsars with observations. Furthermore, we hope that the $3 + 1$ split worked out in Section 4 will encourage other research groups to perform numerical simulations in TMS theories. This may lead to studies of phenomenological interest, such as investigations of dynamical multi-scalarization in neutron star binaries and evolutions of binary black-hole systems in the presence of non-trivial scalar field backgrounds.

Acknowledgments

Appendix A. Spherical and hyperboloidal target spaces

In TMS theory [13], the scalar field $\varphi^A(x^\mu)$ is an application from the space-time manifold $\mathcal{M}$ to the target-space manifold $\mathcal{T}$. This target-space manifold is Riemannian, and its metric is denoted by $\gamma_{AB}(\varphi^C)$. The dimensionality of $\mathcal{T}$ (i.e. the number of scalar fields) is N. Since one-dimensional manifolds are necessarily flat, the simplest non-trivial case is $N = 2$. Furthermore, the simplest two-dimensional manifolds are the maximally symmetric ones, i.e. spherical, hyperbolic and flat spaces. In these spaces, the curvature radius $\hat{r} > 0$ is constant; the Ricci scalar is $\mathcal{R} = 2/\hat{r}^2$ for spherical space, $\mathcal{R} = -2/\hat{r}^2$ for hyperbolic space, and $\mathcal{R} = 0$ for flat space. For convenience we define $\mathfrak{r} = \hat{r},\, i\hat{r}$ for spherical and hyperbolic spaces, respectively, so that the Ricci scalar has the form $\mathcal{R} = 2/\mathfrak{r}^2$ in both cases.

Here we derive the expression for the target-space line element $\gamma_{AB}d\varphi^A d\varphi^B = 2\gamma d\varphi d\bar{\varphi}$ in terms of the complexified scalar field $\varphi = Z + iW$ for the spherical and hyperbolic cases; the result is Eq. (2.16) in the main text.

Spherical target space

The 2-sphere can be defined from its embedding in a three-dimensional Euclidean space of coordinates (x, y, z) through the equation

$$x^2 + y^2 + z^2 = \hat{r}^2 \,. \tag{A.1}$$

It can be parametrized in polar coordinates, defining $\varphi^{A'} = (\Theta, \Phi)$, where:

$$x = \hat{r}\sin\Theta\cos\Phi, \qquad y = \hat{r}\sin\Theta\sin\Phi, \qquad z = \hat{r}\cos\Theta \,. \tag{A.2}$$

The target-space metric in these coordinates is

$$\gamma_{A'B'} = \begin{pmatrix} \hat{r}^2 & 0 \\ 0 & \hat{r}^2 \sin^2 \Theta \end{pmatrix} . \tag{A.3}$$

This frame has undesirable features: in the flat-space limit $\hat{r} \to \infty$ the metric diverges, and the kinetic term in the action (4.1) [where for simplicity we set $V(\Theta, \Phi) = 0$]

$$S = \frac{1}{4\pi G_\star} \int d^4x \sqrt{-g} \left[\frac{R}{4} - \frac{1}{2} g^{\mu\nu} \hat{r}^2 \left(\partial_\mu \Theta \partial_\nu \Theta + \sin^2 \Theta \partial_\mu \Phi \partial_\nu \Phi \right) \right] \tag{A.4}$$

diverges as well. Moreover, the polar frame is not the most suitable for numerical implementation, because it has coordinate singularities at the boundary of the open intervals $0 < \Theta < \pi$, $0 < \Phi < 2\pi$ where the coordinate system is defined. To fix this problem we perform a stereographic projection from the north pole of the sphere (which is the only point of the manifold not covered by this chart) to the plane $\varphi^A = (Z, W)$ tangent to the south pole:

$$Z = \frac{2\hat{r}}{\hat{r} - z} x = 2\hat{r} \frac{\sin \Theta}{1 - \cos \Theta} \cos \Phi , \tag{A.5}$$

$$W = \frac{2\hat{r}}{\hat{r} - z} y = 2\hat{r} \frac{\sin \Theta}{1 - \cos \Theta} \sin \Phi . \tag{A.6}$$

With this projection the equator is mapped to the circle $Z^2 + W^2 = 4\hat{r}^2$; the upper and lower hemispheres are mapped to the exterior and interior of this circle, respectively, and the north pole is mapped to infinity. Using $\sin \Theta / (1 - \cos \Theta) = \cot(\Theta/2)$, the complex field $\varphi = Z + iW$ is written in a more compact form as

$$\varphi = 2\hat{r} \cot(\Theta/2) e^{i\Phi} . \tag{A.7}$$

In the coordinate frame $\varphi^A = (Z, W)$ the target-space metric is

$$\gamma_{AB} = \frac{(1 - \cos \Theta)^2}{4} \delta_{AB} = \frac{\hat{r}^4}{[(Z^2 + W^2)/4 + \hat{r}^2]^2} \delta_{AB}; \tag{A.8}$$

note that $(Z^2 + W^2)/4 + \hat{r}^2 = 2\hat{r}^2/(1 - \cos \Theta)$. In terms of the complex field φ, $\delta_{AB} d\varphi^A d\varphi^B = d\varphi d\bar{\varphi}$, therefore $\gamma_{AB} d\varphi^A d\varphi^B = 2\gamma d\varphi d\bar{\varphi}$ (note that we denote $\gamma = \gamma_{a\bar{b}}$, because a, b can only take the value 1), and

$$\gamma = \frac{1}{2} \left(1 + \frac{\varphi \bar{\varphi}}{4\hat{r}^2} \right)^{-2} . \tag{A.9}$$

Hyperbolic target space

The two-dimensional hyperbolic space of two sheets can also be defined from its embedding into $\mathbb{R}^{1,2}$ with coordinates (x, y, z) through the equation

$$-x^2 - y^2 + z^2 = \hat{r}^2 . \tag{A.10}$$

It can be parametrized in terms of $\varphi^{A'} = (\Theta, \Phi)$ as

$$x = \hat{r} \sinh \Theta \cos \Phi , \qquad y = \hat{r} \sinh \Theta \sin \Phi , \qquad z = \pm \hat{r} \cosh \Theta . \tag{A.11}$$

The target-space metric in these coordinates is

$$\gamma_{A'B'} = \begin{pmatrix} \hat{r}^2 & 0 \\ 0 & \hat{r}^2 \sinh^2 \Theta \end{pmatrix} . \tag{A.12}$$

As in the case of spherical space (see above) the metric diverges when $\hat{r} \to \infty$, and the kinetic term in the action diverges as well. Therefore we perform a stereographic projection from the point at the top of the lower branch to the plane $\varphi^A = (Z, W)$ tangent to the bottom of the upper branch. With this projection, the upper branch is mapped to the interior of the circle $Z^2 + W^2 = 4\hat{r}^2$, and the lower branch is mapped to the exterior of this circle. The stereographic mapping reads

$$Z = \frac{2\hat{r}}{z + \hat{r}} x = 2\hat{r} \frac{\sinh \Theta}{\cosh \Theta + 1} \cos \Phi , \tag{A.13}$$

$$W = \frac{2\hat{r}}{z + \hat{r}} y = 2\hat{r} \frac{\sinh \Theta}{\cosh \Theta + 1} \sin \Phi . \tag{A.14}$$

for the upper branch, and

$$Z = \frac{2\hat{r}}{-z - \hat{r}} x = 2\hat{r} \frac{\sinh \Theta}{\cosh \Theta - 1} \cos \Phi , \tag{A.15}$$

$$W = \frac{2\hat{r}}{-z - \hat{r}} y = 2\hat{r} \frac{\sinh \Theta}{\cosh \Theta - 1} \sin \Phi \tag{A.16}$$

for the lower branch. The complex field $\varphi = Z + iW$ is then $\varphi = 2\hat{r} \tanh(\Theta/2) e^{i\Phi}$ for the upper branch, and $\varphi = 2\hat{r} \coth(\Theta/2) e^{i\Phi}$ for the lower branch.

In the coordinate frame $\varphi^A = (Z, W)$ the target-space metric is

$$\gamma_{AB} = \frac{(1 \pm \cosh \Theta)^2}{4} \delta_{AB} = \frac{\hat{r}^4}{[-(Z^2 + W^2)/4 + \hat{r}^2]^2} \delta_{AB} \tag{A.17}$$

where the upper (lower) sign refers to the upper (lower) branch; note that $-(Z^2 + W^2)/4 + \hat{r}^2 = 2\hat{r}^2/(1 \pm \cos \Theta)$. In terms of the complex field φ, then, the target-space metric is $2\gamma d\varphi d\bar{\varphi}$ with

$$\gamma = \frac{1}{2} \left(1 - \frac{\varphi\bar{\varphi}}{4\hat{r}^2} \right)^{-2} . \tag{A.18}$$

Field equations for two-dimensional spherical and hyperbolic spaces

In summary, the expressions (A.9), (A.18) for the target-space metric in the (two-dimensional) spherical and hyperbolic cases can be written in the form of Eq. (2.16), i.e.

$$\gamma = \frac{1}{2} \left(1 + \frac{\varphi\bar{\varphi}}{4\mathbf{r}^2} \right)^{-2} , \tag{A.19}$$

where $\mathbf{r} = \hat{r}$ for a spherical space, and $\mathbf{r} = i\hat{r}$ for a hyperbolic space. In the coordinate frame $\varphi^A = (Z, W)$ the target-space metric is

$$\gamma_{AB} = \frac{\mathbf{r}^4}{[(Z^2 + W^2)/4 + \mathbf{r}^2]^2} \delta_{AB} \tag{A.20}$$

for both the spherical and hyperbolic space. Therefore, Eqs. (A.19), (A.20) describe a spherical space if $\mathbf{r}^2 > 0$, an hyperbolic space if $\mathbf{r}^2 < 0$. The limit $\mathbf{r} \to \infty$ yields

flat space. If $\mathfrak{r} \to \infty$ and the scalar field is restricted to real values, one recovers the single-scalar case.

The Christoffel symbols are:

$$\gamma^Z_{\ ZZ} = -\tfrac{2Z}{\mathfrak{r}^2+Z^2+W^2}, \quad \gamma^W_{\ ZZ} = \tfrac{2W}{\mathfrak{r}^2+Z^2+W^2}, \quad \gamma^Z_{\ ZW} = -\tfrac{2W}{\mathfrak{r}^2+Z^2+W^2},$$
$$\gamma^W_{\ WW} = -\tfrac{2W}{\mathfrak{r}^2+Z^2+W^2}, \quad \gamma^Z_{\ WW} = \tfrac{2Z}{\mathfrak{r}^2+Z^2+W^2}, \quad \gamma^W_{\ ZW} = -\tfrac{2Z}{\mathfrak{r}^2+Z^2+W^2}. \tag{A.21}$$

In terms of the complex field φ, writing explicitly the indices a, b in $\gamma_{a\bar{b}}$ (which can only take the value 1) we get

$$\gamma^{\bar{c}}_{\ a\bar{b}} = \frac{1}{2}\partial_\varphi \log \gamma = -\frac{\bar{\varphi}}{4\mathfrak{r}^2 + \bar{\varphi}\varphi}, \qquad \gamma^c_{\ a\bar{b}} = \frac{1}{2}\partial_{\bar{\varphi}} \log \gamma = -\frac{\varphi}{4\mathfrak{r}^2 + \bar{\varphi}\varphi}. \tag{A.22}$$

The Ricci tensor and Ricci scalar of the target space are $\mathcal{R}_{AB} = \mathfrak{r}^{-2}\delta_{AB}$ and $\mathcal{R} = 2\mathfrak{r}^{-2}$, respectively.

Replacing the expression of the metric (A.18) and of the Christoffel symbols (A.22) in Eqs. (2.14) and (2.15) with $V(\varphi) = 0$ we find the field equations for a maximally symmetric two-dimensional target space, i.e. Eqs. (2.17) and (2.18).

Appendix B. Solar System constraints

The weak-field limit of TMS theories has been worked out in [13]. Specializing these results to the theory constructed in the body of the text, and rewriting them in complex notation, one finds that the gravitational constant measured in a Cavendish experiment is given by

$$G = G_\star A_\infty^2 (1 + \bar{\kappa}_\infty \kappa_\infty), \tag{B.1}$$

where the subscript ∞ denotes evaluation at $\varphi_\infty = 0$ and we defined the complex function $\kappa(\varphi, \bar{\varphi})$ as in Eq. (2.19). Using Eq. (2.20), one finds that $\kappa_\infty = 2\alpha^*$.

It is straightforward to show that the post-Newtonian parameter γ_{PPN} reads [13]

$$\gamma_{\text{PPN}} - 1 = -\frac{2\bar{\kappa}_\infty \kappa_\infty}{1 + \bar{\kappa}_\infty \kappa_\infty} = -\frac{8|\alpha^*|^2}{1 + 4|\alpha^*|^2}, \tag{B.2}$$

and therefore the Cassini bound $|\gamma_{\text{PPN}} - 1| < 2.3 \cdot 10^{-5}$ [22] implies the constraint

$$|\alpha^*|^2 < 3 \cdot 10^{-6} \tag{B.3}$$

on the coupling constants α^* and $\bar{\alpha}^*$ appearing in Eq. (2.20). Crucially, the one above is a bound on $|\alpha^*|$, whereas $\arg \alpha^*$ is completely unconstrained in the weak-field limit.

On the other hand, the post-Newtonian parameter β_{PPN} reads [13]

$$\beta_{\text{PPN}} - 1 = \frac{\bar{\kappa}_\infty \kappa_\infty \beta_\infty}{2(1 + \bar{\kappa}_\infty \kappa_\infty)^2}, \tag{B.4}$$

where the real-valued function $\beta(\varphi, \bar{\varphi})$ is defined by

$$\beta(\varphi, \bar{\varphi}) \equiv \frac{1}{2}\left(1 + \frac{\bar{\varphi}\varphi}{4\mathfrak{r}^2}\right)\left(\kappa \frac{\partial}{\partial\bar{\varphi}} + \bar{\kappa}\frac{\partial}{\partial\varphi}\right)\log(\bar{\kappa}\kappa). \tag{B.5}$$

Using the definitions above and Eq. (2.20) we obtain

$$\begin{aligned}
\beta_{\text{PPN}} - 1 &= \frac{\alpha^* \alpha^* \bar{\beta}_1^* + 2\alpha^* \bar{\alpha}^* \beta_0 + \bar{\alpha}^* \bar{\alpha}^* \beta_1^*}{(1 + 4\alpha^* \bar{\alpha}^*)^2} \\
&= \frac{2|\alpha^*|^2}{(1 + 4|\alpha^*|^2)^2} \left(\beta_0 + |\beta_1^*| \cos(2\arg\alpha^* - \arg\beta_1^*) \right).
\end{aligned}$$
(B.6)

Finally, the bound $|\beta_{\text{PPN}} - 1| < 1.1 \cdot 10^{-4}$ coming from the combination of Cassini and Lunar Laser Ranging measurements [63] implies a constraint on some combination of the parameters β_0, $|\beta_1^*|$, and $\arg\alpha^* - \frac{1}{2}\arg\beta_1^*$. However, note that if $|\alpha^*| \to 0$ the observational constraint $|\beta_{\text{PPN}} - 1| < 1.1 \cdot 10^{-4}$ is satisfied for any value of β_0, $|\beta_1^*|$ and $\arg\alpha^* - \frac{1}{2}\arg\beta_1^*$, and therefore these parameters are unconstrained by weak-field observations in this limit.

Appendix C. Linearized field equations and scalarization

Here we consider the ST theory defined by Eqs. (2.21) and (2.23) with $\alpha = 0$, which admits GR solutions with $\psi \equiv 0$. We will perturb these GR solutions, and linearize the field equations in the perturbations. This is valid when the amplitudes of the scalar fields are small and consequently the metric back-reaction on the scalar field can be neglected. This approximation is well motivated at the onset of scalarization.

The field equations acquire a particularly simple form when linearized to first order in $Z \equiv \text{Re}[\psi]$ and $W \equiv \text{Im}[\psi]$. In this case, the tensor field equations (2.21) reduce to

$$R_{\mu\nu} = 8\pi G_\star \left(T_{\mu\nu} - \frac{1}{2} T g_{\mu\nu} \right),$$
(C.1)

and therefore the background geometry to $\mathcal{O}(Z, W)$ is described by a GR solution. The scalar-field equation (2.22) becomes

$$\Box Z = -4\pi G_\star (\beta_0 + \beta_1) T Z,$$
(C.2)

$$\Box W = -4\pi G_\star (\beta_0 - \beta_1) T W,$$
(C.3)

where, in this perturbative expansion, the box operator is evaluated on the GR background solution and the trace of the perfect fluid energy-momentum tensor T attains its GR value, i.e. $T = -(8\pi G_\star)^{-1} R = 3P - \rho$. Note that the equations for Z and W decouple in this limit, reducing to the same equation as in the single-scalar case, $\Box\varphi = -4\pi G_\star \beta T \varphi$, but with effective coupling parameters $\beta = \beta_0 + \beta_1$ and $\beta = \beta_0 - \beta_1$, respectively.

In the case of a single scalar, the term on the right-hand side of the scalar equation can be interpreted as an effective mass term (cf. e.g. [1])

$$m_{\text{eff}}^2 = -4\pi G_\star \beta T.$$
(C.4)

Because in typical configurations $T \sim -\rho < 0$, the effective mass squared is negative when $\beta < 0$. This signals a possible tachyonic instability which is associated with an exponentially growing mode and causes the growth of scalar hair in a process known as *spontaneous scalarization* [23], as discussed in the main text. In the case of static compact stars, it turns out that this instability occurs for $\beta \lesssim -4.35$, the threshold value depending only mildly on the equation of state [64–66].

The same reasoning can be applied to Eqs. (C.2) and (C.3). Because the latter are completely equivalent to two copies of a single-scalar equation, scalarization is expected whenever

$$\beta_0 + \beta_1 \lesssim -4.35 \quad \text{or} \quad \beta_0 - \beta_1 \lesssim -4.35 \,. \tag{C.5}$$

Note that these conditions were derived assuming that each scalar field acquires a non-vanishing expectation value independently and by perturbing a static GR solution. In particular, they do not imply that *both* fields scalarize when both conditions (C.5) are satisfied. In fact, biscalarization can be investigated in this perturbative framework by studying the linear perturbations of (say) the scalar field W on the background of a previously scalarized solution where Z has a non-trivial profile.

References

[1] Berti E, Barausse E, Cardoso V, Gualtieri L, Pani P *et al.* 2015 (*Preprint* 1501.07274)
[2] Polchinski J 1998 *String theory* (Cambridge university press)
[3] Duff M J 1994 Kaluza-Klein theory in perspective *The Oskar Klein centenary. Proceedings, Symposium, Stockholm, Sweden, September 19-21, 1994* (*Preprint* hep-th/9410046)
[4] Randall L and Sundrum R 1999 *Phys. Rev. Lett.* **83** 3370–3373 (*Preprint* hep-ph/9905221)
[5] Randall L and Sundrum R 1999 *Phys. Rev. Lett.* **83** 4690–4693 (*Preprint* hep-th/9906064)
[6] Clifton T, Ferreira P G, Padilla A and Skordis C 2012 *Phys.Rept.* **513** 1–189 (*Preprint* 1106.2476)
[7] Jordan P 1959 *Z. Phys.* **157** 112–121
[8] Fierz M 1956 *Helv. Phys. Acta* **29** 128–134
[9] Brans C and Dicke R 1961 *Phys.Rev.* **124** 925–935
[10] Will C M 2014 *Living Reviews in Relativity* **17** 4 URL http://www.livingreviews.org/lrr-2014-4
[11] Bergmann P G 1968 *Int.J.Theor.Phys.* **1** 25–36
[12] Wagoner R V 1970 *Phys.Rev.* **D1** 3209–3216
[13] Damour T and Esposito-Farèse G 1992 *Class. Quant. Grav.* **9** 2093–2176
[14] Kainulainen K and Sunhede D 2006 *Phys.Rev.* **D73** 083510 (*Preprint* astro-ph/0412609)
[15] Albrecht A, Burgess C, Ravndal F and Skordis C 2002 *Phys.Rev.* **D65** 123507 (*Preprint* astro-ph/0107573)
[16] Damour T and Polyakov A M 1994 *Gen.Rel.Grav.* **26** 1171–1176 (*Preprint* gr-qc/9411069)
[17] Damour T and Polyakov A M 1994 *Nucl.Phys.* **B423** 532–558 (*Preprint* hep-th/9401069)
[18] Chiba T, Harada T and Nakao K i 1997 *Prog.Theor.Phys.Suppl.* **128** 335–372
[19] Fujii Y and Maeda K I 2003 *The Scalar-Tensor Theory of Gravitation* (Cambridge University Press)
[20] Horbatsch M and Burgess C 2011 *JCAP* **1108** 027 (*Preprint* 1006.4411)
[21] Sotiriou T P 2014 *Lect. Notes Phys.* **892** 3–24 (*Preprint* 1404.2955)
[22] Bertotti B, Iess L and Tortora P 2003 *Nature* **425** 374
[23] Damour T and Esposito-Farèse G 1993 *Phys. Rev. Lett.* **70** 2220–2223
[24] Freire P C, Wex N, Esposito-Farese G, Verbiest J P, Bailes M *et al.* 2012 *Mon.Not.Roy.Astron.Soc.* **423** 3328 (*Preprint* 1205.1450)
[25] Barausse E, Palenzuela C, Ponce M and Lehner L 2013 *Phys.Rev.* **D87** 081506 (*Preprint* 1212.5053)
[26] Palenzuela C, Barausse E, Ponce M and Lehner L 2014 *Phys.Rev.* **D89** 044024 (*Preprint* 1310.4481)
[27] Shibata M, Taniguchi K, Okawa H and Buonanno A 2014 *Phys.Rev.* **D89** 084005 (*Preprint* 1310.0627)
[28] Sampson L, Yunes N, Cornish N, Ponce M, Barausse E *et al.* 2014 *Phys.Rev.* **D90** 124091 (*Preprint* 1407.7038)
[29] Taniguchi K, Shibata M and Buonanno A 2015 *Phys.Rev.* **D91** 024033 (*Preprint* 1410.0738)
[30] Novak J 1998 *Phys.Rev.* **D57** 4789–4801 (*Preprint* gr-qc/9707041)
[31] Harada T, Chiba T, Nakao K i and Nakamura T 1997 *Phys.Rev.* **D55** 2024–2037 (*Preprint* gr-qc/9611031)
[32] Herdeiro C A R and Radu E 2014 *Phys.Rev.Lett.* **112** 221101 (*Preprint* 1403.2757)

[33] Herdeiro C A R and Radu E 2015 *Int. J. Mod. Phys. D* **24** 1542014 (*Preprint* `1504.08209`)
[34] Bekenstein J 1995 *Phys.Rev.* **D51** 6608–6611
[35] Sotiriou T P and Faraoni V 2012 *Phys.Rev.Lett.* **108** 081103 (*Preprint* `1109.6324`)
[36] Heusler M 1995 *Class.Quant.Grav.* **12** 2021–2036 (*Preprint* `gr-qc/9503053`)
[37] Chrusciel P T, Costa J L and Heusler M 2012 *Living Rev.Rel.* **15** 7 (*Preprint* `1205.6112`)
[38] Heusler M 1996 *Black Hole Uniqueness Theorems* (Cambridge: Cambridge University Press)
[39] Sotiriou T P 2015 (*Preprint* `1505.00248`)
[40] Will C M and Zaglauer H W 1989 *Astrophys. J.* **346** 366
[41] Mirshekari S and Will C M 2013 *Phys.Rev.* **D87** 084070 (*Preprint* `1301.4680`)
[42] Yunes N, Pani P and Cardoso V 2012 *Phys.Rev.* **D85** 102003 (*Preprint* `1112.3351`)
[43] Horbatsch M and Burgess C 2012 *JCAP* **1205** 010 (*Preprint* `1111.4009`)
[44] Healy J, Bode T, Haas R, Pazos E, Laguna P *et al.* 2012 *Class.Quant.Grav.* **29** 232002 (*Preprint* `1112.3928`)
[45] Berti E, Cardoso V, Gualtieri L, Horbatsch M and Sperhake U 2013 *Phys.Rev.* **D87** 124020 (*Preprint* `1304.2836`)
[46] Damour T and Esposito-Farese G 1996 *Phys.Rev.* **D54** 1474–1491 (*Preprint* `gr-qc/9602056`)
[47] Misner C W, Thorne K S and Wheeler J A 1973 *Gravitation* (W. H. Freeman, San Francisco)
[48] Moroianu A 2007 *Lectures on Kähler Geometry* (Cambridge University Press)
[49] Hartle J B 1967 *Astrophys.J.* **150** 1005–1029
[50] Hartle J B and Thorne K S 1968 *Astrophysical Journal* **153** 807
[51] Horbatsch M, Silva H O, Gerosa D, Pani P, Berti E, Gualtieri L and Sperhake U in preparation
[52] Ponce M, Palenzuela C, Barausse E and Lehner L 2015 *Phys.Rev.* **D91** 084038 (*Preprint* `1410.0638`)
[53] Alcubierre M 2008 *Introduction to 3+1 Numerical Relativity* (Oxford University Press)
[54] Salgado M 2006 *Class.Quant.Grav.* **23** 4719–4742 (*Preprint* `gr-qc/0509001`)
[55] Salgado M, Rio D M d, Alcubierre M and Nunez D 2008 *Phys. Rev.* **D77** 104010 (*Preprint* `0801.2372`)
[56] Sotani H 2010 *Phys.Rev.* **D81** 084006 (*Preprint* `1003.2575`)
[57] Doneva D D, Yazadjiev S S, Stergioulas N and Kokkotas K D 2013 *Phys.Rev.* **D88** 084060 (*Preprint* `1309.0605`)
[58] Pani P and Berti E 2014 *Phys.Rev.* **D90** 024025 (*Preprint* `1405.4547`)
[59] Yagi K and Yunes N 2013 *Science* **341** 365–368 (*Preprint* `1302.4499`)
[60] Yagi K and Yunes N 2013 *Phys.Rev.* **D88** 023009 (*Preprint* `1303.1528`)
[61] Alsing J, Berti E, Will C M and Zaglauer H 2012 *Phys.Rev.* **D85** 064041 (*Preprint* `1112.4903`)
[62] Berti E, Gualtieri L, Horbatsch M and Alsing J 2012 *Phys.Rev.* **D85** 122005 (*Preprint* `1204.4340`)
[63] Williams J G, Turyshev S G and Boggs D H 2009 *Int.J.Mod.Phys.* **D18** 1129–1175 (*Preprint* `gr-qc/0507083`)
[64] Harada T 1997 *Prog.Theor.Phys.* **98** 359–379 (*Preprint* `gr-qc/9706014`)
[65] Novak J 1998 *Phys.Rev.* **D58** 064019 (*Preprint* `gr-qc/9806022`)
[66] Silva H O, Macedo C F B, Berti E and Crispino L C B 2015 *Class. Quant. Grav.* **32** 145008 (*Preprint* `1411.6286`)